Surface and near-surface runoff processes in peatland catchments.

Adam Threlfall Hartley

Submitted in accordance with the requirements for the degree of

Master of Science by Research

The University of Leeds

School of Geography

November 2021

The candidate confirms that the work submitted is his own and that appropriate credit has been given where reference has been made to the work of others.

Acknowledgements

Thanks go to my supervisors Prof. Andy Baird, Dr. Paul Morris, and Dr. Mark Smith, for their assistance in the completion of this work and their continued support through what has been an incredibly difficult year. Special thanks also go to Tom Sim and Richard Fewster for their help with fieldwork.

I would also thank my family and partner, Eve-Elodie, for their continued support throughout the last year. I thank my friends and in particular, Beth Mroz for being extremely supportive and allowing me to stay at hers whilst I completed lab work and Ewan Richardson who was always willing to help with coding.

And finally, thanks go to the JBA Trust, the BHS, and the Environment Agency whose studentship award was gratefully received and helped cover the costs of tuition for this degree.

This thesis is dedicated to my Grandparents; Oma and Opa, my Great Aunt Eileen and Great Uncle Leslie and lastly my Aunty Pat and Uncle Neil, all of whom sadly passed away in the last 2 years. I miss them all immensely every day.

Abstract

Blanket peatlands are the most extensive peatland environments in the UK and exhibit flashy responses to rainfall (Evans et al., 1999; Acreman and Holden, 2013). Near-surface and surface flows dominate, produced by saturation-excess and percolation-excess mechanisms, resulting in rapid runoff. Previously, coupled models with explicit representations of subsurface and overland flow, have been used to simulate peatland hydrological processes. These models assume a clear boundary between the subsurface and surface; however, unlike most mineral soils, peatlands lack a distinct surface. This study suggests that the surface constitutes more of a transition zone, comprising a tangle of porous vegetation, meaning that flow is perhaps akin to stormflow in the upper peat, rather than true overland flow. Thus, it is unclear if flow here is Darcian or should be described by a surface flow equation such as the Chézy equation. Laboratory flume experiments were undertaken on two peat samples to simulate flow in the near-surface region, using the data collected to empirically test the Darcian model, DigiBog_Hydro, and determine if a Darcian approach can be used to represent these rapid flows.

The flume experiments showed that for the scenarios with higher water levels, a flashier hydrograph was produced indicating that flow in the near-surface region is responsible for the rapid response of peatlands. DigiBog_Hydro was successful in producing reasonable replications of the observed data, with discharge hydrographs that were comparable in terms of magnitude and shape, and the modelled water tables showing similar patterns of input attenuation as the flume. The differences in the data (lags and absolute water-table heights) are thought to be a result of model 'short-circuiting' and initial model draining, respectively. These data show that the incorporation of a Darcian overland flow layer within DigiBog_Hydro is effective at modelling the rapid quasi-overland flow in the peat near-surface, indicating that a single representation of flow could be used in future and scaled up to entire peatland catchments.

Table of Contents

List of Figures

List of Tables

Abbreviations

Abbreviation	Term
CH_4	Methane
CO_2	Carbon Dioxide
DBD	Dry Bulk Density
DBH	DigiBog_Hydro
Diri	Dirichlet Boundary Condition
DOLF	Darcian Overland Flow
GHGs	Greenhouse Gases
LOESS	Locally Weighted Least Squares Regression
MAE	Mean Absolute Error
Neu	Neumann Boundary Condition
N_2O	Nitrous Oxide
NS	Notional Surface
NSE	Nash-Sutcliffe Efficiency
PT	Pressure Transducer

Symbols

Symbol	Name	Dimensions	Units
A	Cross-sectional Area	L^2	cm^2
C	Chézy Coefficient	$L^{1/2}\ T^{-1}$	$cm^{1/2}\ s^{-1}$
d	Flow Thickness	L	cm
E	Evaporation	$L\ T^{-1}$	$cm\ s^{-1}$
H/h	Hydraulic Head/Water-Table Elevation	L	cm
i	Model Timesteps	-	-
j	Model Spatial Steps (cells)	-	-
K	Hydraulic Conductivity	$L\ T^{-1}$	$cm\ s^{-1}$
n	Number of data points	-	-
P	Rainfall	$L\ T^{-1}$	$cm\ s^{-1}$
Q	Discharge	$L^3\ T^{-1}$	$cm^3\ s^{-1}$
$\mathrm{Q_m}$	Modelled Discharge	$L^3\ T^{-1}$	$cm^3\ s^{-1}$
$\mathrm{Q_o}$	Observed Discharge	$L^3\ T^{-1}$	$cm^3\ s^{-1}$
$\overline{\mathrm{Q_o}}$	Mean Observed Discharge	$L^3\ T^{-1}$	$cm^3\ s^{-1}$
s	Specific Yield	Dimensionless	-
S	Energy Slope	L/L	cm/cm
t	Time	T	s
T	Transmissivity	$L^2\ T^{-1}$	$cm^2\ s^{-1}$
U	Flow Velocity	$L\ T^{-1}$	$cm\ s^{-1}$
u_c	Unit-conversion Factor	Dimensionless	-
vol	Volume	L^3	cm^3/mL
x	Horizontal distance in flow direction	L	cm
Y	Average Flow Depth	L	cm

1. Introduction

1.1. Blanket peatlands

This study concerns the measurement and modelling of water flow in the near-surface of blanket peatlands. Overall, peat covers ~3% of the global land surface (Xu et al., 2018) and ~12% of the UK land surface (UKCEH, n.d.). Peatlands provide many ecosystem services, including carbon storage (holding ~one third of organic carbon in the terrestrial biosphere) and sequestration (Gorham, 1991; Turunen et al., 2001; Frolking and Roulet, 2007; Yu et al., 2010); water quality regulation (Dubuc et al., 1986; Bragg, 2002); biodiversity protection (Bragg, 2002); fuel and recreational services (Page and Baird, 2016; Artz et al., 2019). However, many UK peatlands are now degraded (Worrall et al., 2009; Evans et al., 2017) resulting in a loss of ecosystem services and the emission of greenhouse gases (GHGs) (Leifeld et al., 2019); namely carbon dioxide (CO_2) and nitrous oxide (N_2O) (Couwenberg et al., 2011; Tiemeyer et al., 2016; Evans et al., 2021), with methane (CH_4) emission being more complex (Rosenberry et al., 2006; Turetsky et al., 2014). ~87% of all peat cover in the UK is blanket peat and is typically found in upland headwater catchments (Natural England, 2010; Ballard et al., 2011). These peatlands are now widely considered substantial, highly saturated, source areas for flooding, with rapid system responses (Burt, 1995; Evans et al., 1999; Ala-aho et al., 2017).

Although not as well understood as mineral soils, studies show that blanket peatland runoff is dominated by flow in the upper peat (hereon termed the near-surface) and over the surface, with high streamflow recorded when water-tables are high (Evans et al., 1999; Holden and Burt, 2003a). Furthermore, high water-tables mean there is reduced storage available, with incident rainfall running off quickly and accentuating flooding (Acreman et al., 2011; Lewis et al., 2012; Acreman and Holden, 2013; Allott et al., 2019).

1.2. Peatland response to rainfall

The flood response of peatland-fed rivers and streams depends on how water flows through and across blanket peats. These flows further depend on the properties of the peatland soil, namely hydraulic conductivity (*K*), and the degree of initial saturation.

1.2.1. Peat soil properties

Peat soils are typically described as having two functional layers, the acrotelm (upper layer) and the catotelm (lower layer) – coined the diplotelmic model (Ingram, 1978). The acrotelm is a low density and high *K* layer consisting of fresh and relatively undecomposed litter, whilst the catotelm is more decomposed, humified and; is denser, less porous and has a lower *K* (Figure 1.1) (Holden and Burt, 2003b; 2003c; Evans and Warburton, 2007). *K* defines the ability of water to flow through the soil and is dependent on pore size, structure, and connectivity, with higher *K* meaning faster flow and vice versa. Figure 1.1 shows the relationship between *K* and degree of decomposition, highlighting the initial rapid change with increased decomposition. Also, despite the acrotelm's supply of fresh litter keeping *K* high, it is occasionally aerated which enhances aerobic decomposition, meaning that *K* declines and density increases quickly with depth, into the catotelm which is near-permanently beneath the water-table, resulting in slower (anaerobic) decomposition (Holden and Burt, 2003c; Evans and Warburton, 2007, pp.30-32).

Figure 1.2(b) highlights the conceptual diplotelmic profile outlined above, including the changes in *K* and decomposition rate with depth. An alternative model is also presented (Figure 1.2(c)) which includes a mesotelm (Clymo and Bryant, 2008), where the water-table actively fluctuates, and divides the acrotelm into two layers, with the pectotelm describing the living layer of vegetation (Clymo cit. Morris et al., 2011). These layers are also often above the water-table and are highly porous meaning water flow here is likely to be extremely fast, depending on the slope. However, the *K* profile shown (Figure 1.2(d)) does not account for any *K* variation

in deeper peat (e.g., Clymo, 2004), or the impact of quasi-saturation - which relates to the presence of air and gas bubbles blocking hydrologically effective pores, thus reducing *K* and available subsurface storage (Faybishenko, 1995; Beckwith and Baird, 2001; Baird and Waldron, 2003; Rosenberry et al., 2006).

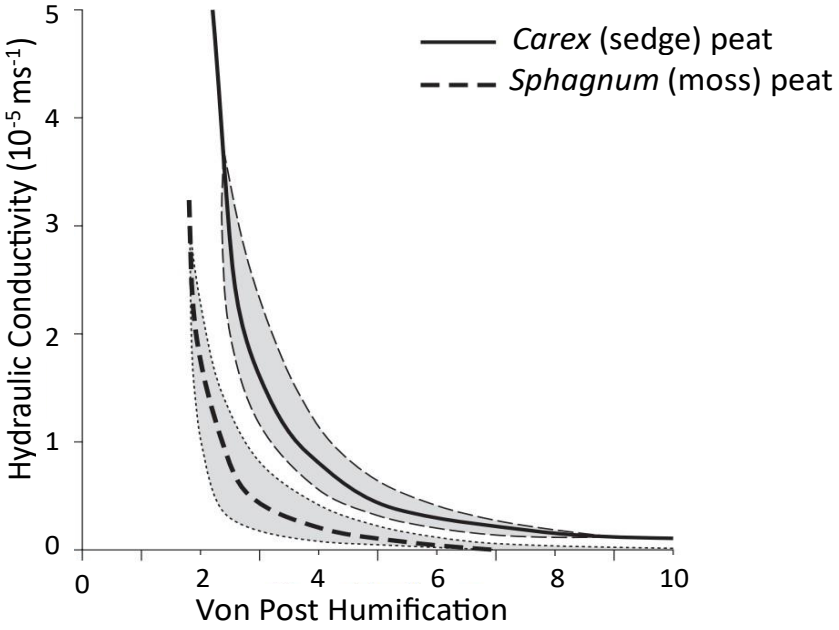

Figure 1.1. Degree of humification and hydraulic conductivity in *Sphagnum* and *Carex* peat. After Egglesmann et al. (1993) (cit. Evans and Warburton, 2007, p.29).

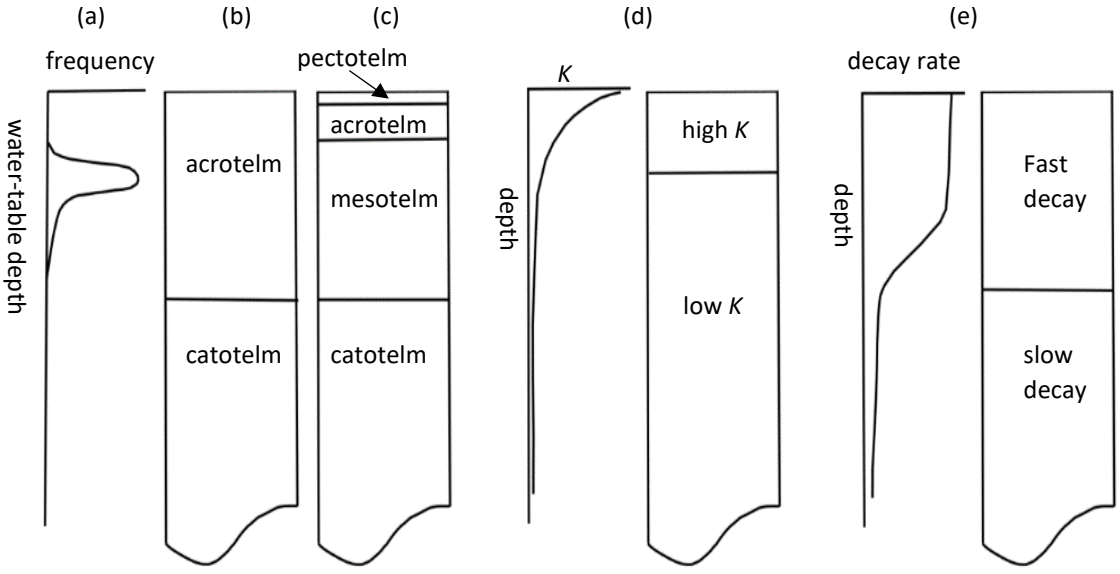

Figure 1.2. Conceptual peat profiles showing: (a) water-table depth distribution; (b) Ingram's (1978) diplotelmic model; (c) the polytelmic model; (d) ranges in hydraulic conductivity throughout the diplotelmic profile; (e) changes in decay rate throughout the diplotelmic profile. From: Morris et al. (2011).

1.2.2. Runoff processes

Peatlands are described as hydrologically "flashy" and show rapid responses to rainfall which raises the often already high water-tables and produce steep, near-symmetrical storm hydrographs, with short lags and quick recession (Burt, 1992; Evans et al., 1999; Holden, 2005; Holden, 2006; Gao et al., 2018). The flows responsible for this rapid response typically happen in the upper portions of the peat profile and occur when the water-table rises into these upper high *K* layers, with little flow occurring when water-tables are low.

1.2.2.1. The water-table

The water-table is the location where groundwater and atmospheric pressures are equal (Marinas, 2009), and its position exerts significant control on much of the runoff produced in peatland catchments. It is true, in a sense, that peatlands hold water and prevent it being released downstream due to the low *K* at depth, and so, their inability to readily drain maintains the high levels of saturation and a relatively high water-table that is near the surface (Brown et al., 2015; University of Leeds Peat Club, 2017). The lack of baseflow sustained in slightly ephemeral peatland-fed streams, when water-tables are low between storm events, is indicative of the restricting properties of deep peat (*K*), meaning that any flow produced in the deep subsurface is very low compared to flows produced in the upper peat (Price, 1992; Evans et al., 1999; Holden, 2005).

Evans et al. (1999) and Daniels et al. (2008) both report maintenance of high water-tables (within 5 cm of the surface) for 93% and 70% (for their intact site) of their monitoring periods of 3 and 1.5 years, respectively. The highest streamflow discharges correlate with high saturation and rainfall, accounting for ~78% of total discharge during the 3-year study period at Trout Beck (North Pennines, UK) (Evans et al., 1999). Therefore, it is clear that discharge is dominated by runoff in the near-surface region of peat when water-tables are high, with surface

ponding likely caused by saturation-excess mechanisms from rainfall falling on already saturated soil.

1.2.2.2. Saturation-excess flow

Typical runoff pathways are shown in Figure 1.3. Saturation-excess flow is the result of rainfall falling on saturated soils (high water-tables) and infiltrating in, quickly filling the remaining pore spaces, causing the already high water-tables to rise to the surface and runoff to occur. Moreover, stream hydrograph evidence shows that high discharge correlates with high water-tables in peatland catchments (Figure 1.4), with Evans et al. (1999) reporting that during a 3-year period, there were no high discharge events where water-tables were concurrently low, indicating that infiltration-excess flow (Hortonian overland flow - Horton, 1933; 1945) is unlikely, but may occur in localised parts of a catchment.

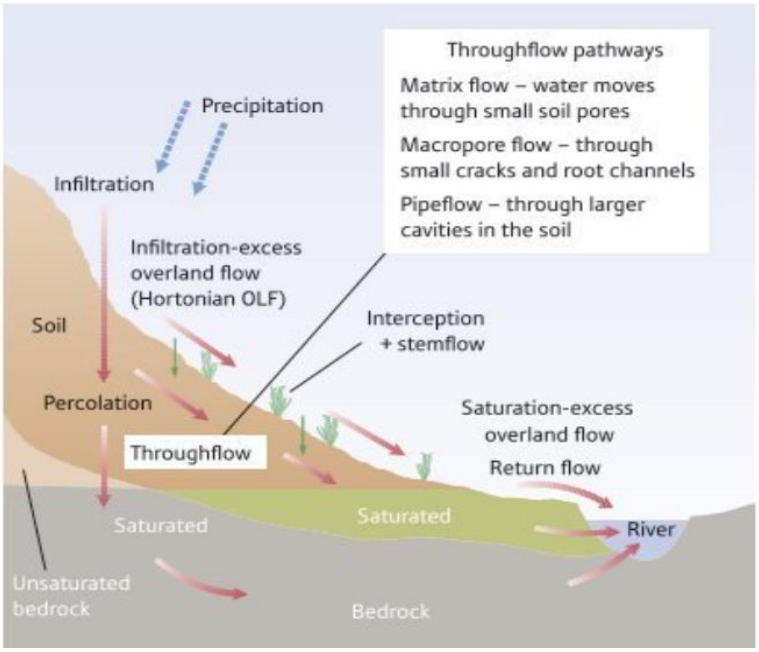

Figure 1.3. Runoff pathways. From: Holden (2017), p.476.

Saturation-excess flow can occur during smaller, low intensity events and continue after rainfall has stopped. It is particularly prevalent on slopes with thin soils (restricted storage capacity), shallow gradients and at the base of slopes (return flow) (Holden, 2017), because of

the reductions in hydraulic gradients impeding drainage (Holden and Burt, 2003a; Gao et al., 2018). Water flowing across the surface is then subject to the influence of roughness (vegetation) which may slow the flow (Holden et al., 2008; Grayson et al., 2010; Gao et al., 2015; 2016).

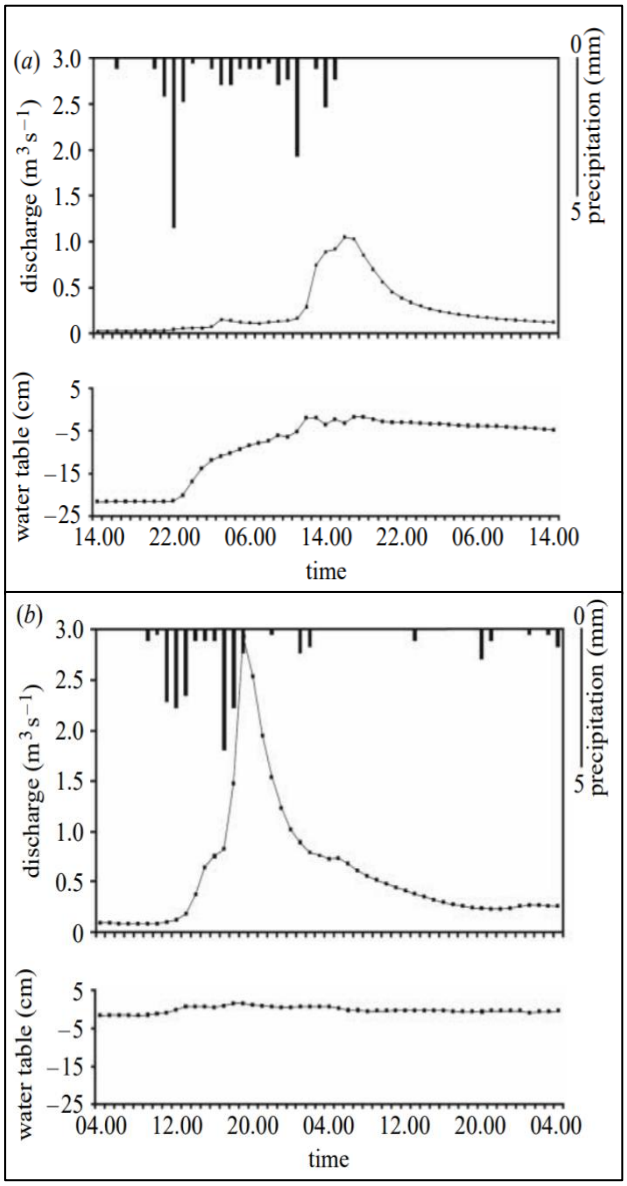

Figure 1.4. Hydrographs and water-table elevation of the Trout Beck catchment (North Pennines, UK) showing the runoff response to rainfall when the water-table is low (a), highlighting slow water-table recharge; and when the water-table is high (b), showing a quicker runoff response. From: Holden (2005).

1.2.2.3. Throughflow

Throughflow is water flow that occurs within the peat and encompasses matrix flow, pipeflow and macropore flow, the latter dominating in the near-surface of peatlands (Baird, 1997b; Holden et al., 2001; Holden, 2009). In addition to the near-permanent saturation of the catotelm, resulting in saturation-excess flow, the low porosity and permeability of deeper peat means that water infiltrating into the near-surface becomes restricted and cannot transfer below (water infiltrating quicker than it can percolate down), producing percolation-excess runoff in this near-surface region (Holden et al., 2001; Holden and Burt, 2002b; Holden, 2009). Macropores control *K* here, with the majority of flow occurring in pores greater than 1 mm, and can produce ~30% of total runoff (Baird, 1997a; Holden et al., 2001). Despite the considerable thickness of the catotelm, the low *K* means that throughflow there is limited (Baird et al., 1997; Holden and Burt, 2003a), with Clymo (2004) reporting that at their site, peat basal velocities were as low as 0.6 mm $year^{-1}$. These findings corroborate those of Evans et al. (1999) where streamflows of <0.5 $m^3 s^{-1}$ occurred 71% of the time across 3 years at Trout Beck (North Pennines, UK), but only accounted for 22% of total discharge, indicating restricted subsurface flow. Meanwhile, Lapen et al. (2005) found that 90% of groundwater flow occurred in the acrotelm, with catotelm flow largely being vertical, again highlighting the dominance of near-surface flow. After dry periods (e.g., summer), incident rainfall does readily infiltrate in, creating more flow in the shallow peat, before the eventual but reduced development of concurrent stormflow and overland flow when the water-tables rise, resulting in a delayed hydrograph (Holden and Burt, 2002b). In contrast, after wet periods (e.g., spring) water-tables are high resulting in a larger flood peak with little delay (Figure 1.4) (Ogawa and Male, 1986; Holden, 2005), indicating that even with low water-tables, flow is low due to the restricted drainage of the catotelm. The dominance of near-surface contributions to runoff is shown in Table 1.1 from a peatland catchment in Upper Wharfedale (Yorkshire Dales, UK).

Pipeflow can bypass sections of peat, enabling transfer of water from deeper sections and providing a preferential flow mechanism. Soil pipes are a type of macropore that are larger than 10 mm and can account for 10-14% of flow and are particularly dominant in recessional or low flow (up to 30%) (Holden and Burt, 2002a; Holden, 2005; Smart et al., 2012). Therefore, they are perhaps less important in producing an immediate response to rainfall than flow produced by percolation-excess and saturation-excess mechanisms, but still play an important role in the system.

Table 1.1. Runoff (%) collected in troughs from peat layers in Upper Wharfedale (Yorkshire Dales, UK), December 2002 – December 2004. Data does not include the sampling of pipeflow and only show matrix throughflow. From: Holden (2005).

Peat Layer (depth, cm)	Percentage runoff from hillslope
0-1	74
1-8	21
8-20	5
>20	<0.01

1.3. Peatland hydrological modelling

Holden and Burt's (2002b; 2003a; 2003b; 2003c) series of studies demonstrated how flow is partitioned in a blanket peatland, highlighting the dominance of saturation-excess flow and near-surface stormflow in producing runoff (Evans and Warburton, 2007, p.44). Modelling these peatland flows is important and useful due to the impact they can have on downstream river flow during storm events. However, modelling of peatlands is perhaps more difficult than in dryland or agricultural land environments with mineral soils, due to little being known on how water flow transitions from the subsurface to the surface.

1.3.1. The peatland surface

Thus far, flows have been discussed with reference to the peatland surface, for example, when separating near-surface stormflow (throughflow) and saturation-excess overland flow. However, unlike many mineral soils, there is a difficulty with identifying a clear surface in blanket peat bogs and so the distinction between these flow regimes is not straightforward. For example, when looking at the profile of a mineral soil, the surface boundary between soil and vegetation is usually quite clear, whereas in intact and actively forming blanket peatlands there is no such clarity. There is a shift from highly humified, compacted catotelm peat to more porous acrotelm peat, but there is no distinct surface at the top. Holden and Burt (2002b) suggest that surface definitions vary between studies, themselves using the first centimetre of intact peat, not considering loose litter as a surface. This study suggests that, instead of a distinct surface, there is more of a thick fuzzy transition zone that is comprised of a tangle of relatively undecomposed and live vegetation (e.g., *Sphagnum* and cotton grass) that is highly porous (Figure 1.5). However, it is unclear if water flow in this zone is Darcian, as in the subsurface.

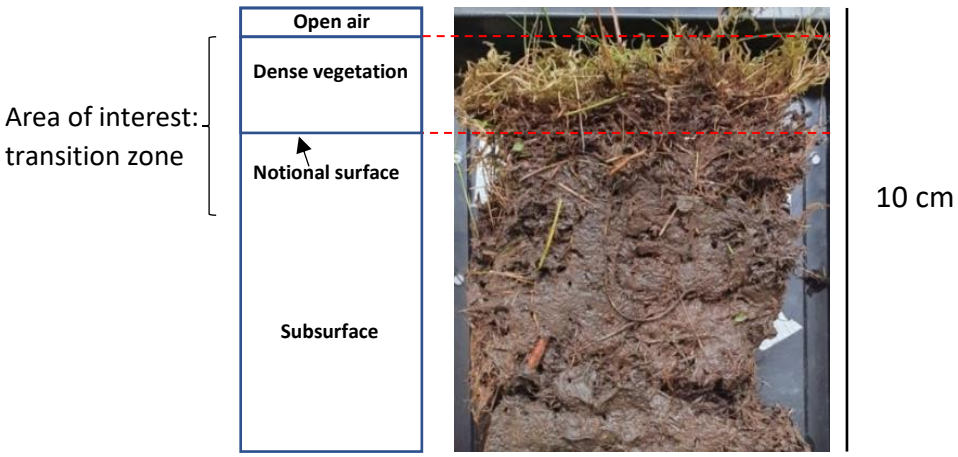

Figure 1.5. Simple schematic and photo of a peat soil cross-section.

1.3.2. Modelling flow

As indicated above, the lack of a surface creates a problem when it comes to modelling the partition of flow, between Darcian matrix throughflow in the subsurface and overland flow on the surface. Flow in a highly porous transition zone at the top of the peat profile could be described as quasi-overland flow, but it is unclear how flow here is represented numerically. It is possible that Darcy's law (eq. 1.1 - Darcy, 1856 cit. Hubbert, 1957), which governs laminar flow through a porous media, is sufficient (as with throughflow in the subsurface) – approximating quasi-overland flow as a diffusion (with high *K* and specific yield (*s*)). Or, if flow is more akin to true overland flow, then a more robust description such as the Chézy equation (eq. 1.2) is required.

(1.1) $$Q = KA\frac{\Delta H}{\Delta x}$$

In equation 1.1 Q is the rate of water flow ($cm^3\ s^{-1}$), *K* is hydraulic conductivity ($cm\ s^{-1}$), A is the cross-sectional area of flow (cm^2), H is hydraulic head (cm), and x is distance in direction of flow (cm).

(1.2) $$U = u_c C\sqrt{YS}$$

In equation 1.2 U is flow velocity ($cm\ s^{-1}$), u_c is a unit-conversion factor, C is the Chézy coefficient (Chézy's C: dimensionless), Y is the average flow depth (cm) and S is the energy slope assumed to be equal to the ground surface slope ($cm\ cm^{-1}$). Darcy's law predicts linear increases in flow with hydraulic gradient whereas overland flow equations, like the Chézy equation, predict non-linear increases in flow.

Whilst there has been considerable work on overland flow (Abrahams and Parsons, 1990; 1991; Abrahams et al., 1994; Dunkerley, 2001; Dunkerley et al., 2001; Dunkerley, 2002) and describing overland flow on arid and semiarid environments (e.g., drylands, semiarid shrub

and agricultural land - Mueller et al., 2007; Thompson et al., 2011; Chen et al., 2013; Crompton et al., 2019; 2020; Crompton and Thompson, 2021), there is comparatively little on peatlands, and so it is unclear how flow in the transition zone/quasi-overland flow can be described mathematically. Overland flow in arid and semiarid environments is generally produced as Hortonion overland flow (Dingman, 1994; Dunkerley et al., 2001; Holden et al., 2008) and is typically described using shallow water (Saint Venant) and flow resistance equations (Crompton et al., 2020). The flow resistance equations used are adopted from those developed for open-channel flows, such as the Chézy equation (see above), the Manning's equation and the Darcy-Weisbach equation (friction factor), which are used in kinematic wave models (Scoging, 1992; Scoging et al., 1992; Parsons et al., 1997; Mueller et al., 2007; Smith et al., 2007; Bond et al., 2020). There has been little work on the modelling of overland flow in peatland environments, with existing work demonstrating the effect of drainage (Ballard et al., 2011; Lane and Milledge, 2013), afforestation (Lewis et al., 2013) and surface cover and vegetation roughness (and vegetation loss) on runoff and peak flows (Holden et al., 2008; Gao et al., 2015; 2016; 2017).

Holden et al. (2008) modelled overland flow in peatlands using an empirical equation and compared these findings to shapes expected from the Darcy-Weisbach equation, relating the friction factor to an effective roughness factor which depends on flow depth, with flow resistance decreasing and velocity increasing once a critical depth was reached. They state, however, that the Darcy-Weisbach equation assumes all elements of roughness are on the bed (surface) and are fully submerged, meaning it may not be applicable for overland flow in peatlands where vegetation is only partially submerged (Holden et al., 2008) or if flow is primarily through a highly porous zone of vegetation. Furthermore, Gao et al. (2015) describe the development of an overland flow model in which the outputs of a subsurface module are input to the surface module (which models overland flow using the Manning's equation), thus requiring a boundary (the surface) between the two modules, splitting the system.

As with Gao et al. (2015), modelling studies in the past have largely focused on the subsurface and surface elements of flow separately, as separate groundwater or overland flow models, that use different equations (Barthel, 2014; Ala-aho et al., 2015). Whilst more fully coupled spatially distributed physically-based models have potential to do this, there is a considerable challenge of parameterising them due to limited data availability and so they are perhaps less applicable (Winter et al., 1998; Barthel, 2014; Barthel and Banzhaf, 2016). In addition, as it is difficult to define where the peatland surface lies, it is possible that there is more of a continuum between the subsurface and surface in peatlands, meaning that flow partitioning can be challenging. Thus, rather than defining a surface and using a coupled model, it seems constructive to model peatlands as one entity, under a single flow representation, making it possible to determine if the system can be modelled this way, in a simpler and more convenient fashion.

Holden and Burt (2002b) found that surface flow on peatlands can often be greater than 1 cm deep but is highly dependent on the definition of the surface as well as surface and soil properties. Thus, it is likely that any overland flow does not fully submerge vegetation but is more likely to flow through it. Little work explicit to peatland hillslopes has been done on this transitional type of flow, but comparison could be made to wetland channel flow and overland flow occurring on wetlands, which is described as flow through partially submerged/fully submerged porous vegetation, where emergent vegetation (such as *Sphagnum* with its branching structure) provides the most resistance to flow through drag (Kadlec, 1990; Leonard and Luther, 1995; Nepf, 1999; Freeman et al., 2000; Copeland, 2000; Nepf et al., 2007; Holden et al., 2008). Kadlec et al. (1981) suggest that this flow could be described with a friction law, including Darcy's law, and report that their studied wetland supports a laminar flow mechanism through the detritus zone, perhaps indicating that Darcy's law may be sufficient at describing flow in blanket peatlands. Furthermore, Choi and Harvey (2014) suggest that flows in wetlands

are characterised as either laminar or transitional but not turbulent, indicating that equations such as the Chézy or Manning's equation are perhaps not applicable (Leonard and Luther, 1995). However, the relevance of these flows to those on peatland hillslopes is questionable because they may have much shallower gradients (<1%) and potentially deeper water levels (Holden et al., 2008).

It may be possible to treat the highly porous transition zone at the top of peatland soils as Darcian, like flows in the subsurface, instead of using a coupled system that has a different representation for flows on the surface. As such, this study uses a combined experimental and numerical modelling approach that compares the response of two types of undisturbed blanket peat to rainfall, considering whether a Darcian treatment is reasonable and applicable in this transition zone by testing an extended Darcian model against the observed experimental datasets.

2. Research aims

The aim of this study is to model near-surface and surface water flow across a peatland slope, using a combined hardware and numerical modelling approach. This work will enable the determination of whether Darcian flow can be used to represent quasi-overland flow that occurs in a system with no defined surface. A Darcian model that could be used to predict peatland hydrological function both at small-scales and over a peatland hillside, using a single flow representation, is presented. This model would provide an alternative to previously used coupled models that may be unsuitable, but also more complex and potentially computationally intensive (e.g., Crompton and Thompson, 2021). This aim is broken down into two objectives which outline the methodology involved in reaching this aim.

- O1: Use hardware models to generate datasets that can be used to test a numerical model that simulates both subsurface and transition-zone flow using Darcy's law.
- O2: Construct numerical model representations of the hardware models and determine if a Darcian (diffusion-type process) model can be used to represent rapid flow in the upper sections of the peat profile (near-surface).

3. Methods

3.1. Methodological overview

A combined hardware and numerical modelling approach is utilised for this study. This approach involves extracting undisturbed samples of peat from a field site and running hardware experimental models on them in a laboratory. A laboratory experimental method bridges the gap between field observation and numerical simulation and has been used in geomorphological studies in the past (e.g., Dunkerley, 2002; Bennett et al., 2015; Lai et al., 2016 and references therein), particularly when investigating smaller-scale processes in a controlled environment (Seeger et al., 2012). The laboratory method is advantageous for this study because it enables modelling scenarios to be devised, and factors, boundary conditions and initial conditions to be controlled and measurements to be made accurately (Kleinhans et al., 2010; Bennett et al., 2015), whilst maintaining the integrity of the field sample (i.e., the sample has not been altered, nor has the peat been 're-packed' in the laboratory), meaning that any processes taking place would be as close to natural as possible.

There are disadvantages with this experimental approach, for example, the samples used were small (<2 m in length), and so laboratory experimentation may not capture all the processes and complexities that naturally occur and could be captured through field experimentation and observation. There is also the difficulty of scaling up the results and applying it to processes that occur over large spatial scales, with the controls put in place also likely to deviate from natural systems (Bennett et al., 2015). However, the trade-offs are deemed to be reasonable for the sake of the simplicity and experimentation enabled. Moreover, a larger sample is difficult to extract and keep undamaged and intact during a field campaign. Field experimentation (e.g., rainfall simulators, see Holden and Burt, 2002b; Dunkerley, 2018; Wolstenholme et al., 2020); on the other hand, whilst capturing the true natural processes that

occur, is difficult to conduct. If an observational approach is utilised instead, it is unlikely that enough natural events will occur over a given timeframe to provide a suitable dataset for testing the Darcian numerical model. Thus, bringing samples into the laboratory is sensible, particularly if the peat sample is undisturbed and is of reasonable length. Therefore, flume tanks of 180 cm length, 10 cm width, 20 cm depth were used to try and capture the processes that occur in the near-surface, to the limit of what was practically possible to extract from the field.

In addition, as blanket peatlands are quite variable, with boggy and fen-like areas present, two end members were required for this study, representing peat from an ombrotrophic bog and a fen-like area, respectively. Once these samples were in flume tanks, four scenarios were investigated in the hardware modelling phase to represent different depths of fast flowing water in the upper peat (near-surface) and transition zone (Figure 1.5).

The numerical modelling phase consists of constructing representations of the hardware models and testing them against the datasets gained from the experimental hardware phase, enabling easy comparison between the two and determining if a Darcian model can represent rapid flow in the near-surface section of the peat.

3.2. Hardware Models

3.2.1. Scenarios

Four hardware model scenarios were run for each flume tank, varying the depth of water flowing in the upper regions of the peat by setting the model initial conditions (starting water level) relative to a notional surface (NS – Figure 1.5). Despite the lack of a clear surface boundary, a NS was required to help model the transition zone and determine how flow is represented. However, identifying an NS was challenging due to the thickness of the transition zone previously described, and so identification of a true surface was unlikely, and the methods should be used with caution in this respect. With this challenge in mind, three methods were

used to identify the NS: 1) investigating the boundary between living (the living layer) and dead vegetation; 2) determining the firmness of the soil and noting whether it is tangled vegetation or peat; and 3) resting one end of a 30 cm long steel rod on the surface of the soil and noting where it rests under its own weight, similar to method 2. Using these methods, it was also possible to map the microtopography of the samples (5 cm intervals). The identified NS was used to set up the four scenarios, which are numbered below. For consistency and repeatability, each scenario was repeated five times. The initial conditions specified were set at the downslope end of the flume tanks due to the 1.5° gradient, on which the tanks were set (to represent a shallowly sloping peatland, where deeper blanket peats commonly form - Charman, 1992; 1995; Parry et al., 2012; 2015), causing a sloping water-table.

1) Set the initial condition to the NS and input a pulse of water through the model.
2) Set the initial condition ~2 cm below the NS and input a pulse of water.
3) Set the initial condition ~1 cm above the NS and input a pulse of water.
4) Set the initial condition to the NS and input a pulse of water, twice the size of the preceding scenarios.

These four scenarios represent a range of starting conditions in the hardware models, based on the water level along the flume, and so the different flow depths required in the models were achieved by adjusting the downstream boundary condition and the inflow size (e.g., scenario 4). The scenarios with the highest initial condition were expected to fill most depressions in the microtopography (i.e., scenario 3) with the water level in scenario 2 expected to be primarily in the subsurface across the flume tanks. The water level set in scenario 4 was expected to fill the same depressions in the microtopography as scenario 1; however, the water-table was expected to rise higher due to the larger inflow. Water-table depth was also expected to increase upslope due to the topographic gradient. By having a range of flow depths simulated

across the scenarios, it was anticipated that flow in the transitional zone could be captured, with these data used to test if Darcy's law provides a suitable representation of these flows.

3.2.2. Site selection

To obtain the peat samples for both hardware models, an appropriate site that possessed the variation in peat required (i.e., an ombrotrophic bog and blanket peat that is more akin to a fen) was selected. The nearest site to Leeds that met these requirements and where permission to sample was obtained was Crawshaw Moss on Ilkley Moor (Figure 3.1). Permission to sample Crawshaw Moss was granted by Bradford City Council and two samples of peat were collected. Two sites: an ombrotrophic bog site (1°51'33.23"W, 53°54'37.31"N) and a fen site (1°51'46.56"W, 53°54'36.78"N) were selected on Crawshaw Moss (Figure 3.2).

Figure 3.1. Crawshaw Moss, Ilkley Moor.

3.2.3. Sample collection

Figure 3.3 shows the sampling extraction locations for both the bog site (Figure 3.3A) and the fen site (Figure 3.3B). The vegetation from where the 'bog' sample was obtained comprised *Sphagnum capillifolium* (Ehrh.) Hedw., *Polytrichum commune* Hedw., *Eriophorum vaginatum* L., *Calluna vulgaris* (L.) Hull., and *Eriophorum angustifolium* Honck. The vegetation at the 'fen' site comprised *Vaccinium oxycoccos* L., *Polytrichum commune* Hedw., *Eriophorum*

vaginatum L. and *Sphagnum capillifolium* (Ehrh.) Hedw. The fen site was also considerably wetter than the bog site, which is perhaps the result of groundwater upwelling, which can both decrease decomposition due to higher water-tables or increase it due to greater nutrient contents. Analysis of dry bulk density and von Post humification indicate that the bog site is more decomposed than the fen site (see section 3.2.8).

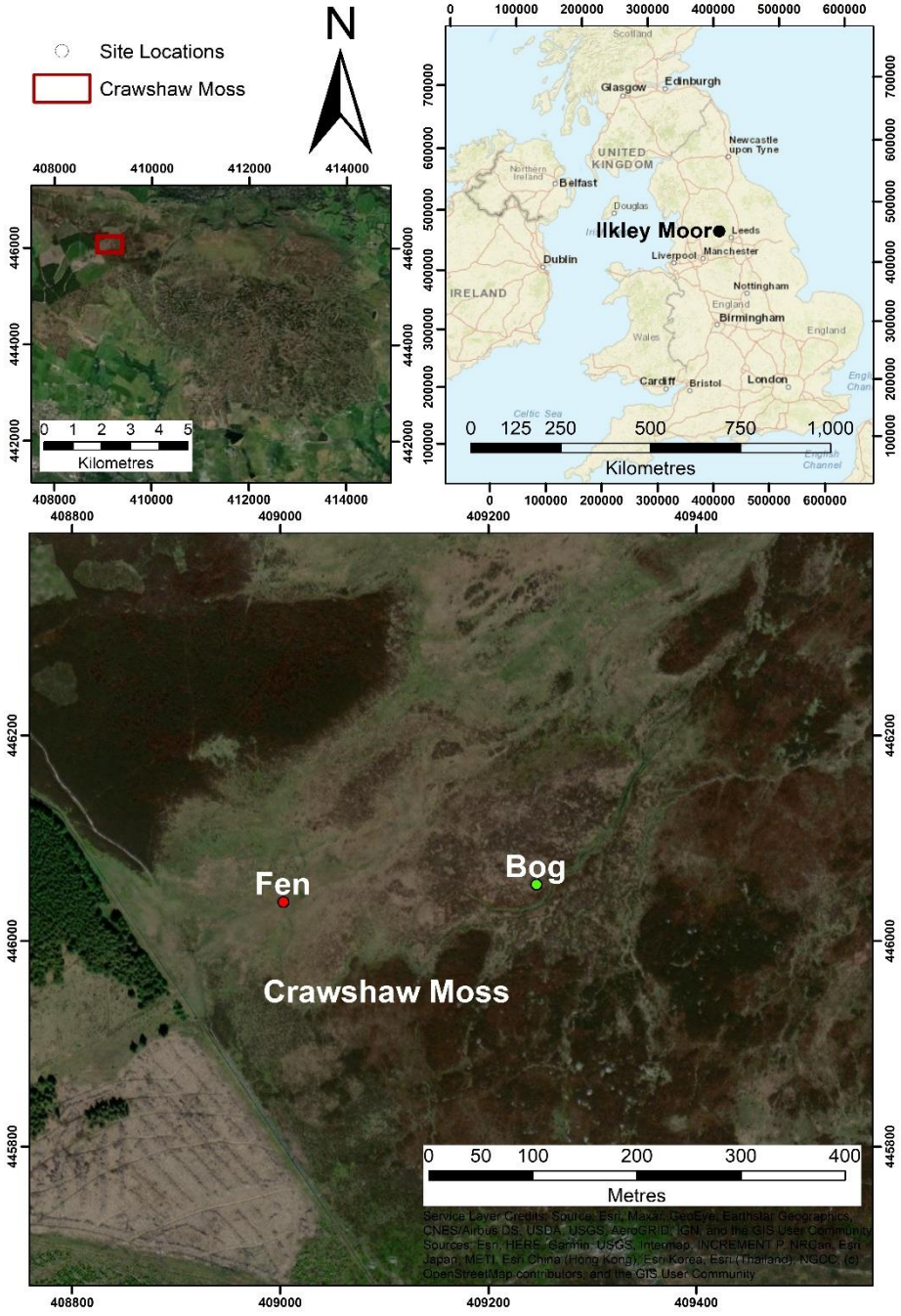

Figure 3.2. Map of Crawshaw Moss on Ilkley Moor, showing the location of both sampling sites.

Figure 3.3. Sampling extraction locations for both sites. A: bog site; B: fen site. Outlines are ~180 cm long.

The extraction method is outlined in Figure 3.4. The empty flume tanks (180 cm long, 10 cm wide, 20 cm deep) were used to mark the edges of the samples and gardening scissors were used to cut a couple of centimetres down into the peat (Figure 3.4A). Planks of plywood were then slotted into these grooves on either side of the tank, to hold the sample in place (Figure 3.4B). Surrounding peat was cut away (using a spade and trowels) from the tanks to create extra space and enable the samples to be evenly cut to greater depths (Figure 3.4B). Once the correct depth was reached, the sample was cut horizontally underneath using the scissors and a flat trowel, separating the sample from the peatland (Figure 3.4C). The sample was then levered out onto the supporting ply and slid into the empty flume tank, ensuring correct orientation (Figure 3.4D). Using this method, it was difficult to ensure the peat was set firmly against the base of the tank, resulting in intermittent gaps between the peat and the tank base. However, the voids were few and not continuous. Once the samples were back in the laboratory, 15 cm of peat on

either end was cut out (Figure 3.5) and replaced with foam inserts to act as the boundary conditions (a Neumann condition representing no flow across the drainage divide (upslope) and a Dirichlet condition representing a set water level at the base of the slope) of the hardware model, as shown in Figure 3.6, resulting in the peat samples used in the models being 150 cm long.

Figure 3.4. Sample extraction methods. A: using the flume tank as a template for extraction; B: plywood planks inserted into grooves alongside sample and removal of material around the sample; C: cutting underneath the sample; D: insertion of sample into flume tank and securing with nylon rods.

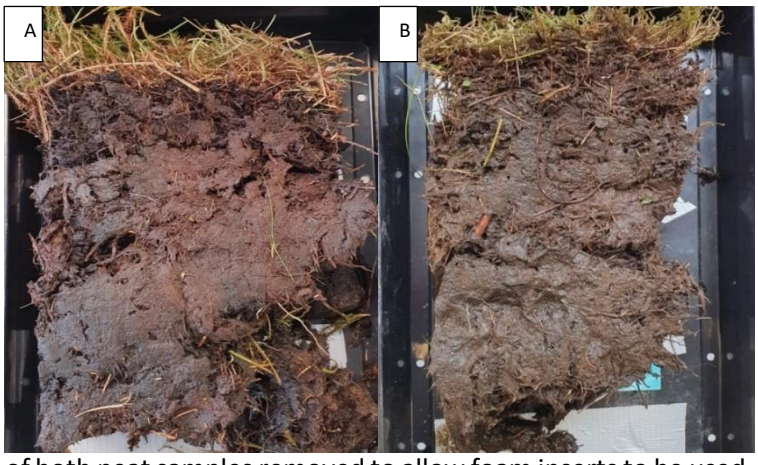

Figure 3.5. Cross sections of both peat samples removed to allow foam inserts to be used at each end. A: ombrotrophic bog site; B: fen-like site.

3.2.4. Experimental setup

Figure 3.6 demonstrates the setup of the flume tank models in the laboratory. The models were set up on apparatus that creates an adjustable ramp whereby the gradient of the slope can be changed, by raising or lowering the clamps, to suit the user's requirements. Box section plastic wells (17 cm long, 8 mm by 8mm external dimensions, with one face removed and 2 mm holes every 1 cm along the face opposite the removed face) were inserted along the side of the tanks at 25 cm intervals (numbered from Well0 to Well150, noting the distance from the upslope end of the peat sample in cm - Figure 3.6). These wells allowed the water-table to be monitored throughout the simulations via video recordings of the runs, which enabled the water-table to be monitored subsequently using a timestep set by the user. Four outflow tubes extend from the flume tanks into the cylindrical outflow collector where a pressure transducer (PT) recorded the water level within the cylinder. These tubes were configured to prevent a siphon effect and any glugging.

For simulating near-surface and surface flows across these peat samples, a syringe pump (Figure 3.6) was installed at the upslope end of each model which inputted a set volume of water into the hardware models at a set rate, that could be adjusted per the users need. Six 100 mL syringes were fixed to each pump with ~95 mL being pumped from each because of the type of syringes used and their configuration on the pump. So, ~570 mL was pumped in total for 57 seconds, at a constant rate of ~10.2 $cm^3 s^{-1}$, for scenarios 1-3, with double this used for scenario 4. These were further calibrated to ensure the volume entering the model was accurate and could be replicated (Figure 3.7), with any variation likely due to small air pockets being present in the syringes and their tubes, despite thorough priming.

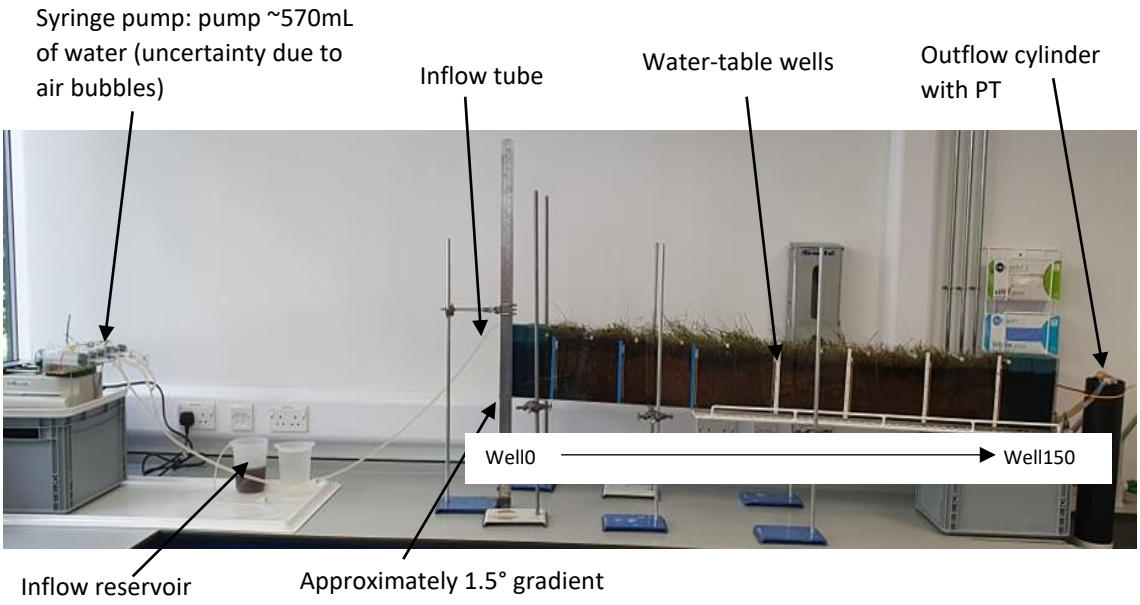

Figure 3.6. Experimental setup of the flume tanks containing the samples of peat. Water-table wells are labelled 0 to 150 as shown. Tank shown is filled with the fen peat. A second tank with the bog peat was setup in the same manner.

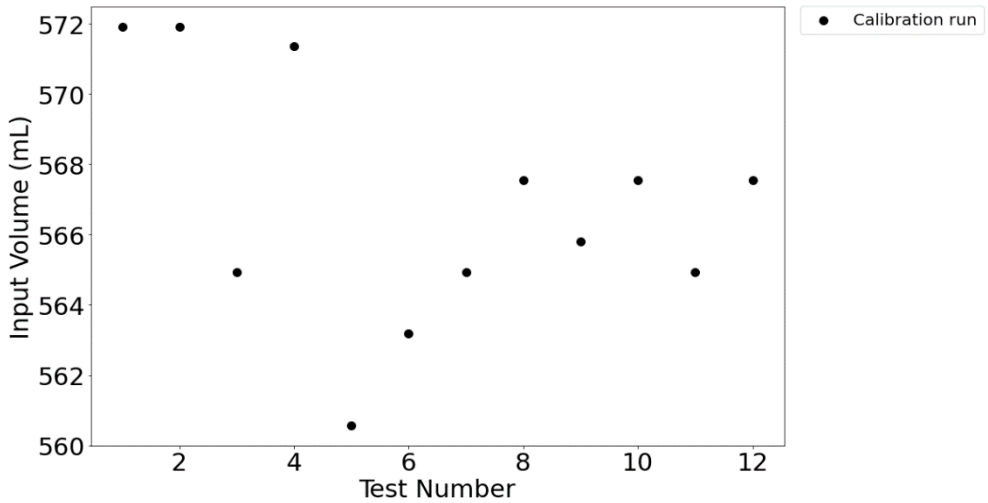

Figure 3.7. Syringe pump test runs.

3.2.5. Setting the initial condition

To set the initial condition, the tanks were first filled with de-ionised water and drained to the required level at the downslope end by setting the level of the outflow tubes to the specified height. The outflow water was also recycled subsequently for the following repeats. Once this level was set, the water levels were left to settle for 30 minutes, for each scenario. For

some scenarios; however, a 30-minute recovery period was not sufficient for the water-table to settle completely – resulting in slight water-table variation between the repeats, with some wells upslope showing higher water-tables than those downslope, indicating that greater recovery times were perhaps required. However, due to time constraints, pragmatism was needed, and a sloping water-table (deeper at the upslope end) may not in fact be representative of a dynamic system (where water is added upslope). The simulations were run after this 30-minute recovery period, with the simulation ending when the water level in the most downslope well (well150) returned to its initial condition.

3.2.6. Data collection and analysis: discharge

Two sets of data were collected for each model run: an outflow discharge and the water-table heights. Discharge was measured using the PT in the outflow cylinder. The raw data from the PT was converted to a water level which was subsequently converted to a volume using a water level to volume calibration. The volume was then differenced between timesteps (vol_2-vol_1) and divided by the time interval to give a volumetric rate (discharge). However, even though the PT had low noise, the estimated discharges showed substantial variation between timesteps (1 s). To reduce the noise and give useable hydrographs, LOESS (locally weighted least squares regression) was used to clean the data. LOESS was implemented, in R, on the volume over time data by fitting multiple regressions in a local neighbourhood to smooth the data, producing a smoothed value of volume for each timestep. Discharge was calculated from the smoothed volume data as above. Two parameters: degree (degree of polynomials) and span (degree of smoothing) within LOESS were calibrated to produce an optimum fit with the volume over time data. A degree of 1 and span of 0.085 were chosen as the optimum values. These parameter values were kept consistent for all LOESS implementations as the size and timing of peak discharge can vary depending on the parameterisation used. LOESS helped produce a smoothed discharge hydrograph for each run and enabled clear comparison between them.

Discharge hydrographs for each scenario and site enabled comparisons to be made between them, helping to determine how water transferred through the fuzzy transition zone to the outlet by comparing peak discharge, lag time and the degree of 'flashiness'. It was also possible to show the spread among the model repeats, helping decide if further water-table analysis was required. Additionally, hydrograph metrics (lag time: time from peak rainfall (centroid) to peak discharge, and time from peak discharge to half the peak discharge (on the falling limb)) were produced to examine the similarities and differences between the scenarios and sites.

3.2.7. Data collection and analysis: water-tables

Water-table heights were recorded using the water-table wells inserted into both hardware models. As noted above, the wells were video recorded to allow for post-simulation analysis of the water-tables, where water-table height was manually extracted from each well. One advantage of this approach is that the user can set a preferred timestep for data extraction depending on how responsive the water-tables are; however, a drawback is that the video is not as clear (a problem exacerbated by dirty perspex and turbid water) as when observing the simulations with the naked eye, meaning there is perhaps an error of +/- 1 mm. This error is particularly noticeable in the most downslope wells where the water-table response to the input is lower than the upslope wells, meaning that they perhaps appear to return to their initial conditions early due to very little movement in the wells. Another limitation stems from the initial water levels in the wells where, despite the recovery time being consistent, some wells displayed slightly different initial levels between repeats, and with wells occasionally showing variation in water-table upslope (i.e., water level in upslope wells was occasionally greater than those downslope). Due to the time-consuming nature of water-table data extraction, the simulation that produced the median discharge hydrograph peak was analysed to examine the differences in water-table response between scenarios. Extraction of the water-table data

allowed for the input signal to be monitored downslope showing how the pulse of water was transformed. Additionally, it was possible to compare the scenarios and tanks and determine the impact the initial condition and peat type had on flow conveyance (water-table peak and lag time) downslope.

3.2.8. Data collection and analysis: dry bulk density and von Post

Further to this, soil dry bulk density (DBD) analysis and von Post humification classification (Rydin and Jeglum, 2006) were undertaken on the peat samples that had been removed from the end of the flume samples (Figure 3.5) to help determine the degree of decomposition. For both analyses, peat cubes with a volume of 8 cm^3 were cut from the samples in 2 cm intervals from the top to the base (e.g., sample 1 is from 0-2 cm and sample 2 is from 2-4 cm, etc). DBD was calculated for both peat samples, first by weighing the crucibles, then the wet soil and then drying the soil in an oven for 24 hours at 80°C. The samples were then left to cool in a desiccator, before final weighing (dry weight). The crucible weights were subtracted from the dry weight and the result was then divided by the volume to get the DBD. The DBD results are shown in Tables 3.1 (bog site) and 3.2 (fen site).

Table 3.1. DBD analysis for the bog site.

Bog Tank	**8 cm^3 samples**
Sample ID	**Dry Bulk Density (g cm^3)**
Bog_0-2	0.099
Bog_2-4	0.126
Bog_4-6	0.166
Bog_6-8	0.150
Bog_8-10	0.189
Bog_10-12	0.243
Bog_12-14	0.226
Bog_14-16	0.135

Table 3.2. DBD analysis for the fen site.

Fen Tank	8 cm^3 samples
Sample ID	**Dry Bulk Density (g cm^3)**
Fen_0-2	0.065
Fen_2-4	0.087
Fen_4-6	0.075
Fen_6-8	0.091
Fen_8-10	0.071
Fen_10-12	0.083
Fen_12-14	0.094
Fen_14-16	0.090
Fen_16-18	0.100
Fen_18-20	0.124
Fen_20-22	0.142

Table 3.3. von Post analysis for the bog site.

Site 1 Tank (Bog site)		
Sample ID	**Classification**	**Description**
Bog_0-2	H2/H3	Clearly see plant structure, springy, yellow-brown water with bits, no ridges when squeezed, no peat escaping between fingers.
Bog_2-4	H3	Structures less distinct than H2, darker water, still fairly springy, no peat substance between fingers.
Bog_4-6	H4	Very dark turbid water, very slight ridges but wouldn't say distinct, more mushy residue, can still make out plant structures.
Bog_6-8	H4	Same as above.
Bog_8-10	H5	Very dark brown turbid water, some peat escapes - slightly more than 1/10 (~1/6) escapes, some ridges.
Bog_10-12	H6	Similar to above but more peat escapes (~1/3) with plant structures clearer in residue.
Bog_12-14	H7	As described in Rydin and Jeglum (2006) with ~1/2 peat escaping.
Bog_14-16	H7	As described in Rydin and Jeglum (2006) with ~1/2 peat escaping.

Von Post classification was undertaken on samples of the same size and extracted using the same technique. For von Post, the plant structures of these samples were inspected, and

the samples were also squeezed with the water colour, proportion of original material remaining, and amount of amorphous material being noted. The samples were then classified into one of the 10 classes (Rydin and Jeglum, 2006). The von Post results are shown in Tables 3.3 (bog site) and 3.4 (fen site).

Table 3.4. von Post analysis for the fen site.

Site 2 Tank (Fen site)		
Sample ID	**Classification**	**Description**
Fen_0-2	H2	Clearly see plant structure, springy, yellow-brown water with bits.
Fen_2-4	H2	Same as above, residue becoming slightly pasty.
Fen_4-6	H3	Distinct plant structures. Darker, browner water, slightly turbid, pasty residue, no substance passing through fingers, no ridges.
Fen_6-8	H3	Same as above.
Fen_8-10	H3	As above but darker and more turbid water - still no ridges or substance passing through. Still pasty residue.
Fen_10-12	H4	Very muddy, turbid and dark water, slightly mushy residue.
Fen_12-14	H5	Plants becoming more indistinct. Dark, turbid water. A little peat escaping and ridges remaining. Mushy residue.
Fen_14-16	H5	As above with a little more peat escaping and more mush.
Fen_16-18	H5	As above.
Fen_18-20	H6	Very muddy, turbid and dark water. Distinct ridges remain. Plant structures clearer in residue. More peat escaping than above but not as much as 1/3.
Fen_20-22	H6	Very similar to above, slightly more peat escaping.

3.3. Numerical Models

A Darcian numerical model was developed to represent both hardware models and discern its suitability for modelling rapid flows that occur in the peat near-surface. The models acted as digital twins, being simplified replicas of the hardware models that were calibrated to

fit the observed datasets from the hardware modelling phase. In addition, the model used was required to be adaptable and able to incorporate a high *K* and *s* layer at the top of the peat column, representing the highly porous transition zone. This layer is hereby denoted the DOLF (Darcian overland flow) layer.

3.3.1. Model selection

The hydrological model DigiBog_Hydro (DBH), a submodel of DigiBog (see Baird et al., 2012; Morris et al., 2012), was selected for the numerical modelling aspect of this project. DBH was primarily selected because the model allows for detailed examination of near-surface processes though the incorporation of multiple soil layers, which also enable vertical and lateral variation in peat properties (*K* and *s*). Therefore, the model is suitable for representing both the peat and the DOLF layer at the top of the peat column, simulating quasi-overland flow as Darcian. Furthermore, DBH can remain stable with a range of *K* profiles, whereas models like Modflow (Harbaugh and McDonald, 1996) - whilst being an industry-standard model - can become unstable with large changes in *K*, which can mean peat layers are often lumped together resulting in inaccurate results (Reeve et al., 2000; Baird et al., 2012). Cells in Modflow also become inactive once drained, meaning they cannot be rewet, introducing another advantage of DBH (Baird et al., 2012). Other models, such as DRAINMOD (Skaggs et al., 1981) and TOPMODEL (Beven and Kirkby, 1979), implement exponential (Skaggs et al., 1981; Beven, 1997; Beven and Freer, 2001a; Metcalfe et al., 2015) and logarithmic *K* profiles (Gao et al., 2015; 2016), which may be an appropriate simplification for some peatlands but not others, and DBHs ability to discretise layers with any profile provides a clear benefit. Moreover, DBHs ability to do this means that peatland heterogeneity and complexities in *K* profiles (Beckwith et al., 2003a; 2003b; Holden and Burt, 2003b; Baird et al., 2008; Lewis et al., 2012; Cunliffe et al., 2013) could potentially be incorporated. Finally, DigiBog has a proven track record of being able to represent peatlands (Baird et al., 2012; Morris et al., 2012; Morris et al., 2015; Garneau et al., 2016; Young

et al., 2020) and so, whilst other models are perhaps capable, DBH's ability to manipulate and discretise peat layers and properties makes it a suitable choice for this project, enabling direct comparison with the hardware models and detailed modelling of the transition zone.

3.2.2. Model description

As noted previously, DBH is a submodel of the model DigiBog and is a 2½ D model, facilitating soil property variation along three dimensions but only flow in both horizontal directions (Baird et al., 2012). The model is built on a range of subroutines that loop through each timestep, calculating water-table height and flow between soil columns (cells). The subroutines start with the calculation of depth-averaged *K* per column, using the transmissivity (*T*) values (product of *K* and depth) to improve efficiency, before calculating the amount of water lost or gained from a column through seepage, rainfall and evaporation, using the harmonic mean of *K* between columns (eq. 3.1). The version of DBH used in this study varied from this with the incorporation of the arithmetic mean of *K* (eq. 3.2), rather than the harmonic mean between cells. The arithmetic mean of *K* was used because the harmonic mean favours the downslope cell. So, for example, if the water table in a downslope cell was lower (in lower *K* layers) than that in an upslope cell, the depth-averaged *K* for that cell would be lower than that of the upslope cell, thus meaning the harmonic mean of *K* between them is low. Therefore, the harmonic mean does not account for the water table in the upslope cell being in the higher *K* layers, resulting in reduced flow between cells and spurious results. Thus, the arithmetic mean, which does not favour the downslope cell, was used.

(3.1) $$\frac{\left(2 * K_{\mathrm{j}}\right) * K_{\mathrm{j+1}}}{K_j + K_{j+1}}$$

(3.2) $$\frac{K_{\mathrm{j}} + K_{\mathrm{j+1}}}{2}$$

Furthermore, instead of rainfall, this study used a pump as input and so rainfall and evaporation are not considered. The final subroutine calculates the new water-table position, accounting for each layer's drainable porosity (*s*), including whether the water table has risen to the surface (top of the peat column). The last two subroutines are based on a finite-difference solution (splitting into spatial and temporal segments) to the Boussinesq equation (eq. 3.3), which is a combination of Darcy's law and the balance equation for 1-D flow (Baird et al., 2012):

$$\frac{\Delta h}{\Delta t} = \frac{\Delta}{\Delta x}\left(\frac{K(d)}{s(d)} d \frac{\Delta h}{\Delta x}\right) + \frac{P(t) - E(h,t)}{s(d)} \quad (3.3)$$

where *h* is water-table elevation (cm) above an arbitrary datum, *t* is time (s), *x* is the horizontal distance (cm), *d* is the thickness of flow (i.e., local height of the water-table above an impermeable base - cm), *K* is the depth-average hydraulic conductivity below the water table (cm s^{-1}), *s* is the drainable porosity (specific yield - dimensionless), *P* is rainfall addition to the water table (cm s^{-1}) minus *E* which is evaporation losses (cm s^{-1}) – not considered here (Baird et al., 2012). As the simulations use slopes of 1.5°, the extended Boussinesq equation was not required (Baird et al., 2012).

3.2.3. Model setup and parameters

Table 3.5 outlines the parameters and their units used in DBH. Layer thickness can be set per soil column and varied throughout the soil profile, with *K* and *s* also able to vary throughout the soil column. The initial water-table level in each cell is the input water-table height and will vary per scenario, as described in section 3.2.1. However, using the raw initial conditions from the hardware models introduced a problem of the model dewatering from the high *K* and *s* layers at the beginning of the model runs. Thus, the model initial conditions were drained for a specified period (1 hour) to reduce this effect and reach a less dynamic state. The change in initial condition here did, however, lead to complications when comparing the modelled water-tables to the observed water-tables, as discussed below. The base altitude

marks the bottom of the hardware model (or beginning of an impermeable mineral layer for a real peatland) and controls the gradient of the slope, using height above a fixed datum (cm). The gradient was set to 1.5° as per the hardware model, inducing a hydraulic gradient by virtue of a topographic gradient. Net rainfall ($precipitation - evaporation$) is incorporated into the base version of DBH. However, instead of rainfall, the input was re-coded (in Fortran) to simulate the syringe pumps adding water at a set rate, for the required time, to a high *K* and *s* cell (representing the foam boundary) at the upslope end of the model (adding water as a depth addition rate per second). In the base version of DBH, the ponding layer depth is the maximum depth at which water can remain on the surface of a cell column and, if exceeded, the water runs off to the model margin or is lost as slow 'overland flow' (Baird et al., 2012). As overland flow is not explicitly represented in the default model, the DOLF layer was incorporated at the top of the soil column, to represent rapid flow in the transition zone as a diffusion.

Table 3.5. DBH Parameters.

Layer thickness	cm
Hydraulic conductivity (*K*)	cm s^{-1}
Specific yield (*s*)	dimensionless (proportion)
Initial water-table level in each cell	cm
Base altitude	cm
Net rainfall	cm $hour^{-1}$
Ponding layer depth	cm

The model can be applied to any peatland shape but must be represented as a grid in which cell columns can be "switched off" when not in use – effectively demarcating the peatland or hillslope boundary. DBH also uses Dirichlet (constant water level) and Neumann boundary conditions (set flow). For this study, a Dirichlet condition was used at the downslope end of the model to mark a constant water level (set to the initial conditions outlined in section 3.2.1),

whilst Neumann boundary conditions marked no flow across the upslope and lateral drainage divides of the model (Figure 3.8 (bottom)). As noted above, the model input was applied to the upper most cell on the slope. The “on” cells represent the peat columns, whilst the “off” cells mark the model domain. The models represent the tanks as a line of 1-D cells, 30 cells long and one cell wide, with each cell being 5 cm in size, covering the 150 cm length of the peat sample. The cell columns were split into layers with the potential to model variation in sample microtopography by altering the thickness of the cell layers. For practical reasons, the model was further simplified whereby the peat thickness did not vary across the slope and was set to the thickness of the peat samples at the downslope end of each tank (15.3 cm for the bog sample and 16.4 cm for the fen sample). A constant thickness still allowed for the correct initial condition to be set as per the scenarios in section 3.2.1, but also avoided over-complicating the model which would be beneficial for scaling up to a hillslope. Furthermore, DBH allows variation in the model parameters (*K* and *s*) within the column layers, and so any *K* and *s* profile can be used. Model run times varied for the hardware modelling, and as such, the same run times were used with DBH for the respective scenarios. A timestep of 0.1 s was used consistently across all modelled scenarios to ensure the model was numerically stable for rapid flows that occur in the near-surface and transition zone. This setup is shown in Figure 3.8, with nine adjacent peat columns, bounded by two or three boundary condition cells. Each peat column has eight interconnected 1D peat layers of a pre-determined thickness, with the DOLF layer at the top set to a thickness of 3 cm for all simulations. The base altitude at the bottom of the cell columns represents the model base (tank base of the hardware models). The cell size and the number of cells can be changed to simulate slopes in higher resolution and/or of a greater size if required; however, with this comes an increase in computational demand and run times.

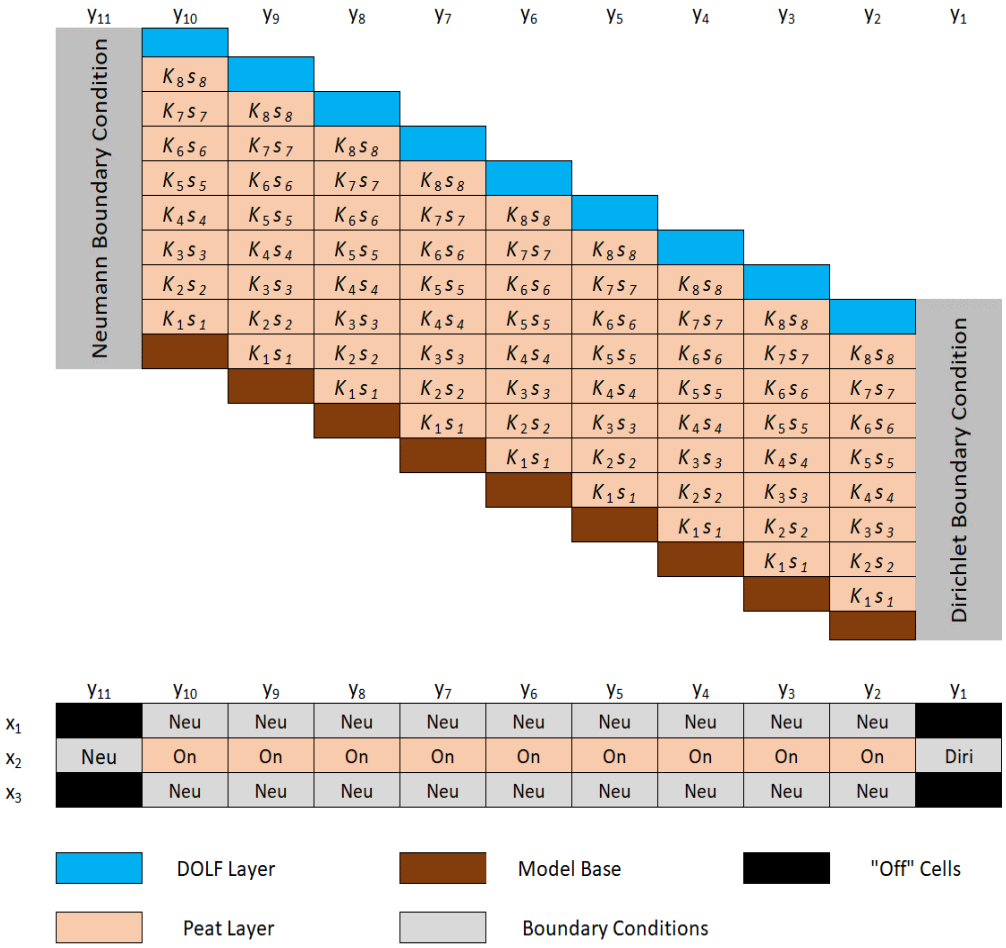

Figure 3.8. Schematic of the DBH setup of the hardware models. Top: side view of DBH for the peat samples; bottom: plan view of DBH for the peat samples. Y direction is along the slope and x direction is across the slope. K_1s_1 represent the *K* and *s* profiles that can be used. Note: more columns were used in the actual model.

3.2.4. Model assumptions and limitations

Like all models, DBH makes several assumptions. Firstly, it is assumed that all water flow beneath the water-table is horizontal – the Dupuit-Forchheimer approximation (McWhorter and Sunada, 1977 cit. Baird et al., 2012) – with a horizontal hydraulic gradient driving flow. The assumption of horizontal flow is taken to be reasonable in peatlands underlain by impermeable strata, which introduces another assumption. However, these assumptions are applicable in the

case of this study as mimicking the hardware model flume tanks means that an impermeable base was required.

Secondly, as shown in Figure 3.8, the peat columns are bounded by boundary conditions, either Dirichlet or Neumann conditions. On either side of the peat cells are Neumann boundary conditions meaning that there is assumed to be no flow in the x direction (across the slope) and flow only occurs in the y direction (down the slope) (see Figure 3.8). This is perhaps not an ideal representation of peatland hillslopes but is reasonable in most cases and for the purposes of this study, it is accepted.

Finally, for the sake of simplicity, the model assumes that there is no change in peat thickness (no microtopography) across or down the slope which may reduce the accuracy in modelling runoff generation (Frei et al., 2010; Frei and Fleckenstein, 2014). It also assumes that there is no lateral variation in K and s parameters, which is unlikely to occur on peatlands (Holden and Burt, 2003b), but is perhaps more reasonable in a small-scale model, as incorporating lateral variation increases complexity.

3.2.5. Model calibration

The primary aim of the numerical modelling component was to produce plausible outputs that are comparable to the hardware model data. However, the model is an abstraction of reality and there is the possibility of multiple parameter sets producing fairly similar outputs: the problem of equifinality and parameter identifiability, where a change in model predictions is difficult to link to a specific parameter (Beven and Freer, 2001b; Pechlivanidis et al., 2011). This study uses an empirical calibration approach with few varying parameters and settings and so the issues described above are less likely here than when calibrating a physically-based model, for instance. The simplified model setup outlined above meant that only the parameters

K and *s* could be altered during calibration, reducing the problem of parameter identifiability but still meaning that multiple parameter sets could produce plausible outcomes.

Using the *K* and *s* parameters, a series of different sets were tested and best fit with the hardware model data was determined semi-quantitatively, both using the discharge and water-table data. However, due to the initial condition being drained at the beginning of each run to reduce the dewatering effect, there was a notable offset in the modelled water-table heights when compared to the observed heights. Consequently, during model calibration, this offset was taken into consideration, along with the shape of the water-table profile and timing of the water-table peak. The discharge hydrograph peak values, timings and shape were also used in calibration. Additionally, objective functions such as the mean absolute error (MAE) and Nash-Sutcliffe Efficiency criterion (NSE) were initially used to determine goodness of fit to the discharge data. MAE was calculated using equation (3.4), where the observed discharge and predicted discharge for each timestep are differenced and the average taken. NSE was calculated using equation (3.5), using variance of errors (eq. 3.5 numerator) and the variance of observations (eq. 3.5 denominator).

(3.4) $$MAE = \frac{\sum_{i=1}^{n} |Q_o^i - Q_m^i|}{n}$$

(3.5) $$NSE = 1 - \frac{\sum_{i=1}^{n} (Q_o^i - Q_m^i)^2}{\sum_{i=1}^{n} (Q_o^i - \overline{Q_O})^2}$$

In equations 3.4 and 3.5 n is the number of data points, i is the timestep, Q_o is the observed discharge at a timestep, Q_m is the modelled discharge at a timestep and $\overline{Q_O}$ is the mean observed discharge.

However, these criteria have pitfalls in their use and were given little weight as small changes in the timing of the rising limb of the discharge hydrograph led to large changes in these criteria, indicating that the overall fit was poor, thus not accounting for size of the peak and

overall shape of the hydrograph. Therefore, the criteria for model success centred on visual comparison between the observed and modelled data, with particular emphasis on discharge peak values, lag times, overall hydrograph shapes and the water-table heights, patterns and profiles of each well.

Table 3.6 Parameter bounds used in calibration.

	K (cm s^{-1})	s (dimensionless)
DOLF layer	8	0.9
Deep peat	0.0001	0.3

It was not feasible to test all the different parameter sets that are possible with this model, with variation in K and s between multiple layers being considered, as well just varying their profiles. Therefore, a more pragmatic approach was used, targeting the variation of parameter sets within identified bounds. These bounds were: no lateral variation in parameters (to keep the model simple), the DOLF layer parameters being constant (high K and s due to the high porosity of the layer, with the values determined experimentally) and the parameters of the deeper peat layers being kept consistently low, as much of the hydrological function of a peatland occurs in the uppermost layers. These bounds are presented in Table 3.6, with the calibration focusing on the layers between the deep peat and the DOLF layer, keeping the values of K and s between these ranges. The values of K and s were altered individually, layer by layer, assuming no lateral variation, with the model outputs semi-quantitively assessed between calibration runs to determine goodness of fit and aid in the identification of the optimum parameter set by observing the result of a parameter change. As noted above, the semi-quantitative assessment of the model parameter sets firstly involved comparison of the observed and modelled discharge peak values, lag times and the overall hydrograph shape (comparing the peakiness and gradients of the rising and falling limbs). Secondly, comparison between the pattern of input attenuation observed in the water tables was undertaken, also

comparing the water-table peak sizes and timings, considering the impact of initial model draining. The thickness of the deep peat layers differed between the model twins due to differences in sample peat thickness in the hardware models (as noted above). Furthermore, it is important to understand that a simpler model, as used here, may produce less good fits than a complex model; however, its simplicity has an advantage in terms of its application, making the model easier to scale up to complete hillslopes. The outputs shown in the results section are produced using the selected parameter sets for both models.

3.2.6. Model simulations and outputs

As the numerical model represented the hardware models outlined in section 3.2, the same set of scenarios were run, using the calibrated parameters, and comparisons were made with the observed outputs to test the model's suitability, noting any differences and similarities. As such, DBH produced discharge outputs, recording the amount of water leaving the model, and water-table height outputs for the same cells (wells) that were sampled in the hardware models. Similar data metrics to the hardware models were utilised for the numerical models too, enabling clear comparison between the discharge data of both models. In addition, the discharge hydrographs and water-table profiles allowed for direct visual comparison between the models to be made.

4. Results

This chapter presents the results from both modelling phases (O1 and O2) and compares the two, providing an indication as to whether DBH's representation of Darcian flow is effective at modelling near-surface peatland hydrological processes.

4.1. Assessing model performance: discharge

When comparing the outputs from the hardware and numerical models, it is clear that the numerical model has provided some good fits to the hardware model data, alongside some discrepancies. The criteria used to determine the degree of fit include the discharge peaks, overall shape of the hydrograph (comparison of the rising and falling limb gradients) and the hydrograph metrics, including lag time and time to half peak (on the falling limb). Figures 4.1, 4.2, 4.3 and 4.4 show the observed discharges and the modelled discharges, for each scenario for the bog and fen site. These figures highlight that overall DBH has provided a good fit with the observed data in terms of discharge peaks and hydrograph shape, for both peat types. The clear difference seen here relates to the lag between the observed and modelled hydrographs.

The modelled peak discharges for scenarios 1 and 2 of the bog model closely matched the median discharge peaks in the observed data, with little difference between them (-0.048 $cm^3 s^{-1}$ and +0.021 $cm^3 s^{-1}$, respectively). Similar fits are observed for these scenarios in the fen model (-0.06 $cm^3 s^{-1}$ and -0.009 $cm^3 s^{-1}$, respectively). Modelled peaks for scenarios 3 and 4 for the bog model both underpredict the observed peaks (-0.323 $cm^3 s^{-1}$ and -0.531 $cm^3 s^{-1}$, respectively). The differences between modelled and observed peaks are greater in scenarios 3 and 4 of the fen model also (-0.450 $cm^3 s^{-1}$ and +0.364 $cm^3 s^{-1}$, respectively). These data are shown in Table 4.1. For each scenario, the modelled hydrograph shapes are comparable with the observed hydrographs (Figures 4.1, 4.2, 4.3 and 4.4). As with the discharge peaks, scenarios 1 and 2 produce modelled hydrographs that follow those of the observed hydrographs well for

both sites (Figures 4.1 and 4.3), with similar gradients to the observed data notable on the rising limbs, although these are not as steep as the observed rising limbs in the bog model. The falling limbs in these scenarios, bar scenario 2 in the fen model (which is faster than the observed falling limb), are slightly more attenuated than in the observed hydrographs, shown by the peak to half discharge times in Table 4.1. By comparison, the modelled hydrograph shapes in the bog model for scenarios 3 and 4 (Figure 4.2) are agreeable but the fit is not as close, with slightly shallower rising limbs than their observed counterparts and slower falling limbs (taking 231 s and 230 s longer for the half discharge peak to be reached, respectively). Although a comparably steep gradient is notable in the modelled rising limb of scenario 3, for the fen model (Figure 4.4), the falling limb is again slightly slower than in the observed hydrograph (by 292 s - Table 4.1). In addition, whilst the modelled peak discharge in scenario 4 of the fen model (Figure 4.4) is greater than the observed peak, the hydrograph shape produced is similar, with a steep rising limb gradient and a falling limb that closely matches the observed data, with little difference between the time to half peaks (the modelled falling limb is 6 s quicker). Differences are also shown in the hydrograph areas for each simulation (Table 4.2), with neither the modelled nor observed areas matching the input volume. However, it must be noted that, due to pragmatic decisions on simulation run time and despite each run ending when well150 returned to its initial condition, discharge does not return to 0 cm^3 s^{-1} for any of the scenarios, meaning that any remaining volume could have been added subsequently.

The lag between the modelled and observed hydrographs is apparent in these figures and the lag times in Table 4.1. However, discounting this lag, the overall good model fit is also apparent, with small differences in peak discharge (for scenarios 1 and 2 particularly) and only slight differences observed in the hydrograph shapes (with the rising limbs particularly well produced), thus indicating that overall, the model was successful in simulating these flows.

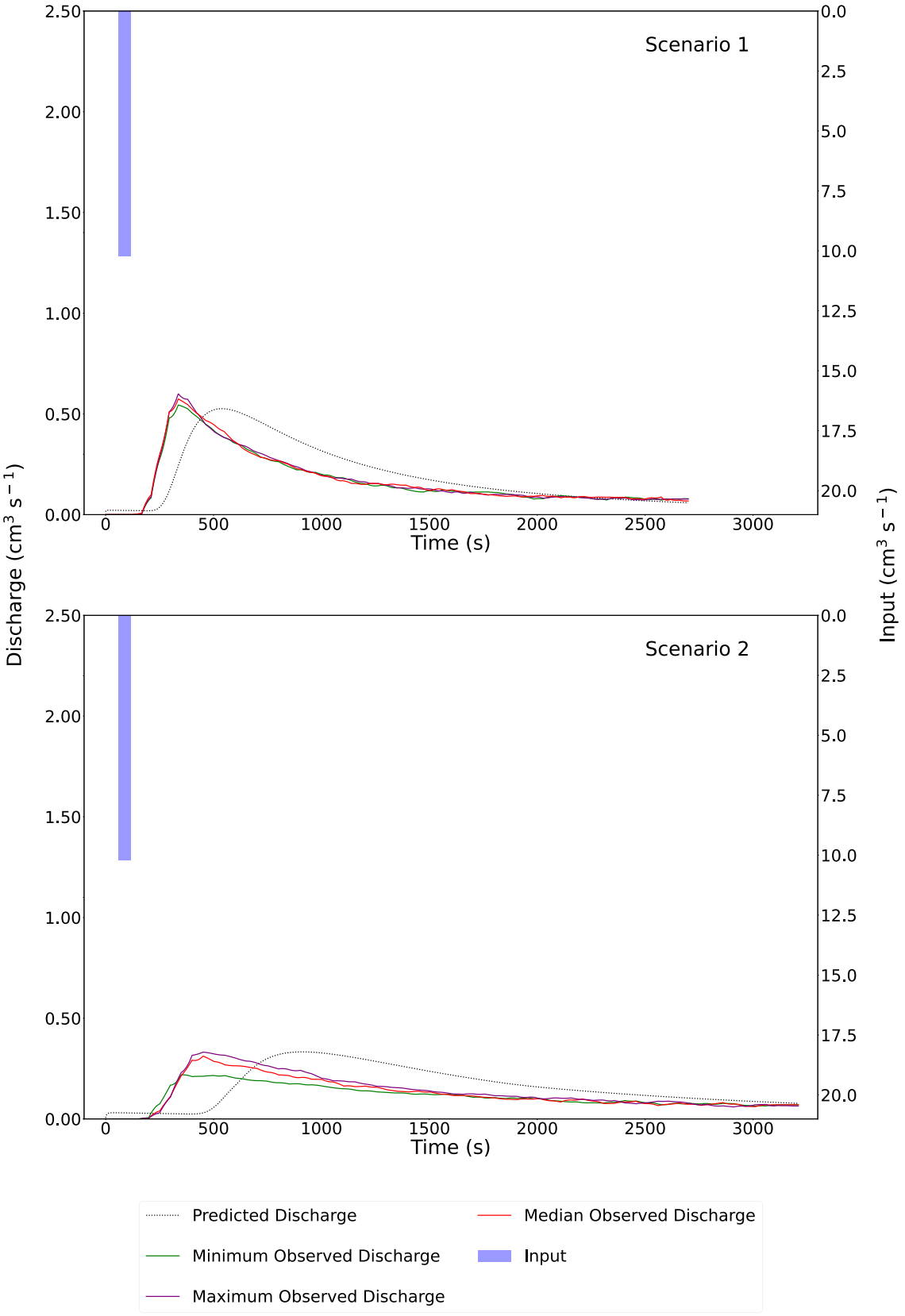

Figure 4.1. Predicted discharges and observed discharges for the bog model for scenarios 1 and 2.

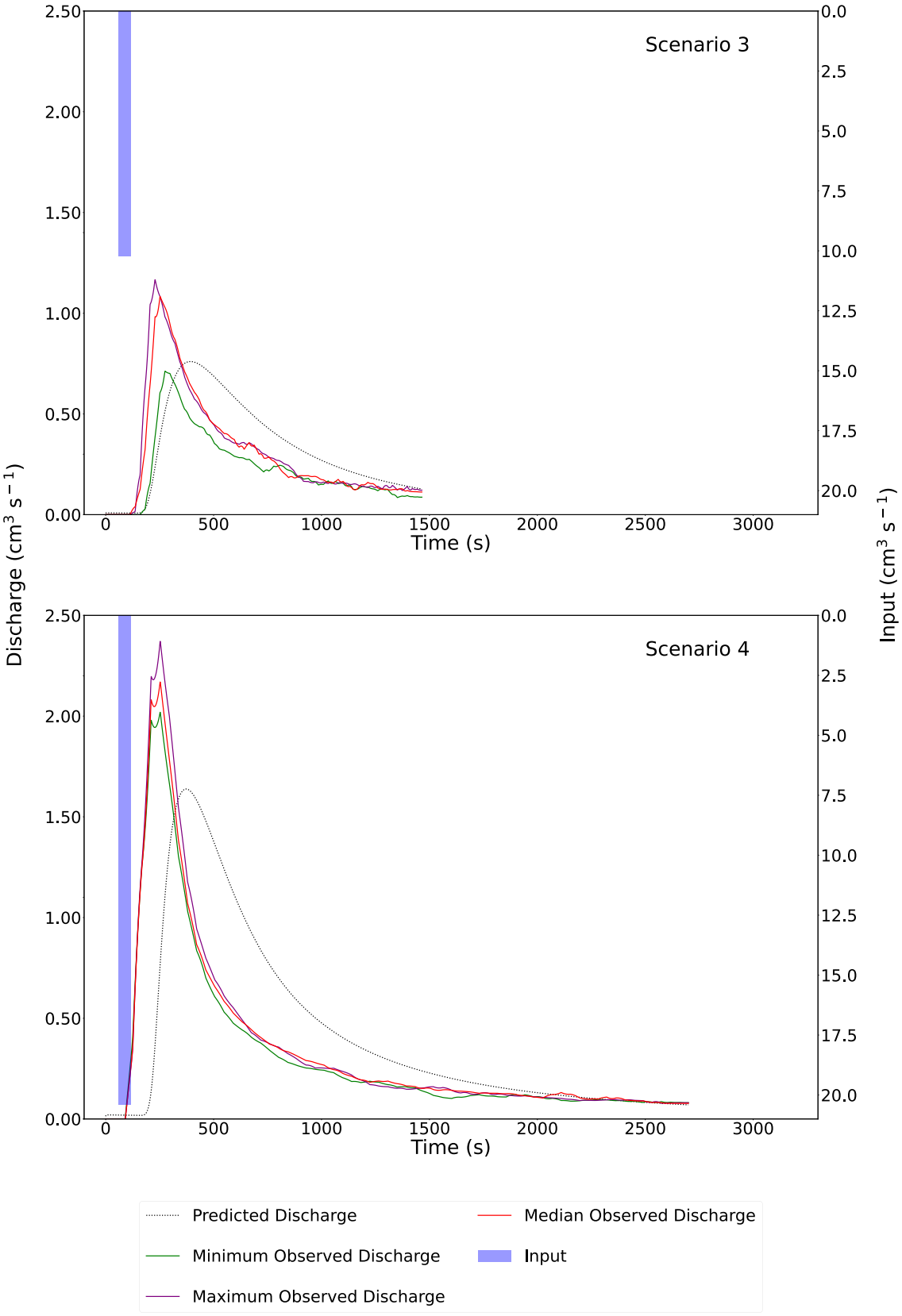

Figure 4.2. Predicted discharges and observed discharges for the bog model for scenarios 3 and 4.

Table 4.1. Observed (median hydrographs) and modelled hydrograph metrics for those in Figures 4.1 to 4.4. The lag time is the time from peak rainfall (centroid) to peak discharge and the time from peak to half peak discharge is the time taken for discharge to reach half the value of the peak on the falling limb.

Site	Scenario	Observed/ Modelled	Peak discharge ($cm^3 s^{-1}$)	Lag time (s)	Peak to half discharge time (s)
Bog	1	Observed	0.574	248	375
		Modelled	0.526	449	607
	2	Observed	0.312	363	812
		Modelled	0.333	823	1022
	3	Observed	1.083	163	191
		Modelled	0.760	304	422
	4	Observed	2.169	163	126
		Modelled	1.638	284	356
Fen	1	Observed	0.545	285	464
		Modelled	0.485	485	666
	2	Observed	0.288	586	1208
		Modelled	0.279	945	1015
	3	Observed	1.186	147	144
		Modelled	0.736	311	436
	4	Observed	1.211	174	368
		Modelled	1.575	293	362

Table 4.2. Observed (median hydrograph) and modelled hydrograph areas (output volume) and total run times.

Site	Scenario	Total Run Time (s)	Observed/ Modelled	Hydrograph Area (Vol = mL)
Bog	1	2700	Observed	468.227
			Modelled	544.201
	2	3210	Observed	400.367
			Modelled	519.077
	3	1465	Observed	446.993
			Modelled	495.776
	4	2700	Observed	938.803
			Modelled	1119.938
Fen	1	3418	Observed	481.211
			Modelled	558.675
	2	2700	Observed	437.304
			Modelled	377.896
	3	1003	Observed	393.845
			Modelled	399.689
	4	2400	Observed	884.512
			Modelled	1079.683

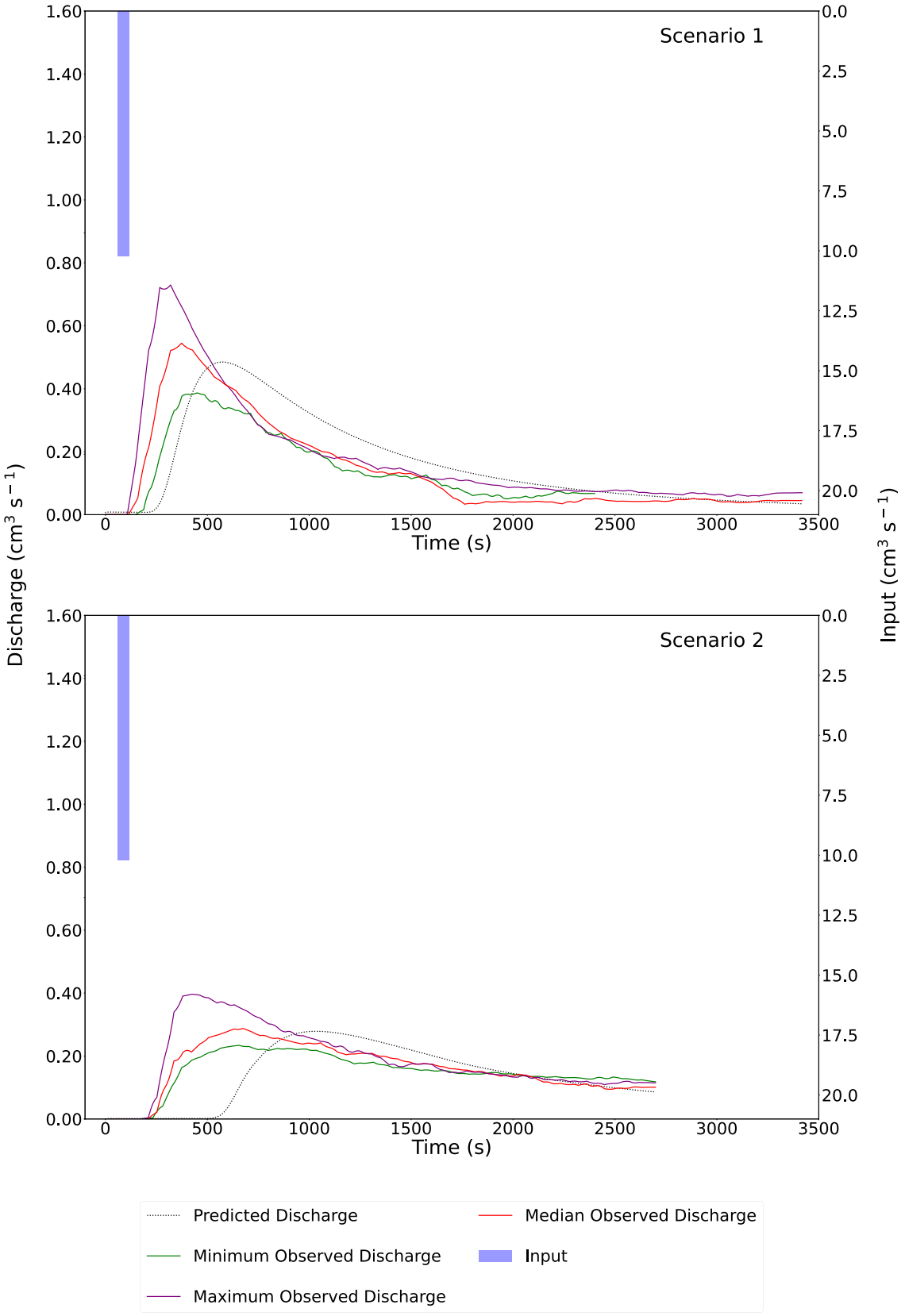

Figure 4.3. Predicted discharges and observed discharges for the fen model for scenarios 1 and 2.

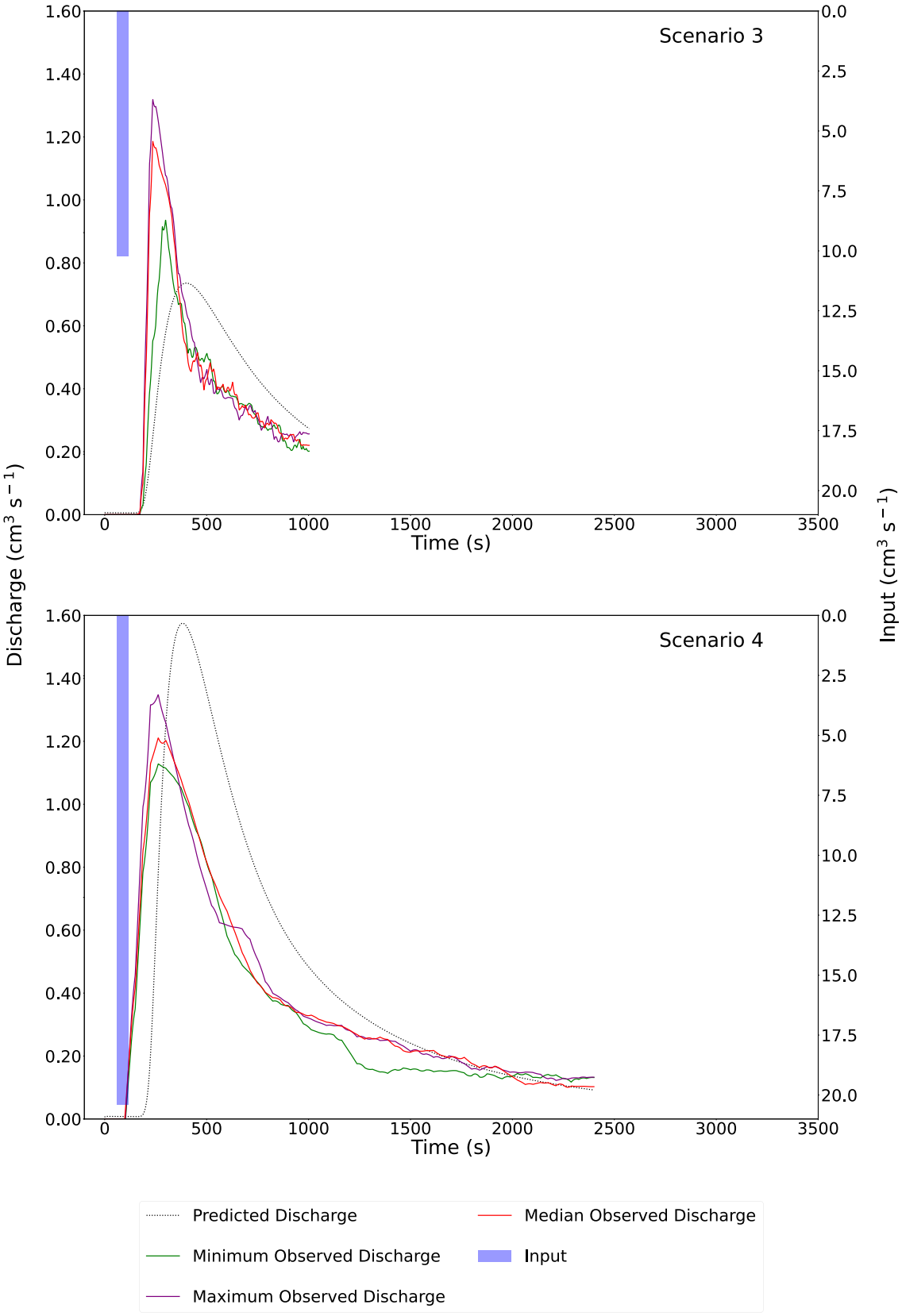

Figure 4.4. Predicted discharges and observed discharges for the fen model for scenarios 3 and 4.

4.2. Assessing model performance: water-tables

Figures 4.5, 4.6, 4.7 and 4.8 show the observed and modelled water-table height data for each scenario and model. A similar pattern in water-table profiles is noticeable for the observed data from both tanks, with scenario 2 having the slowest water-table response to input (slower rise and more attenuated profiles), and scenario 4 having the quickest and more pronounced response, followed by scenarios 3 and 1. Across all scenarios, the response in the two most upslope wells (well0 and well25) are comparable with large peaks and short lag times. The remaining well profiles plot consecutively to the right, showing attenuation of the input signal as water travels downslope, with the peaks reducing in height and becoming more delayed.

Like the modelled discharges, a set of criteria were used to determine the fit of the modelled water-table data. These criteria include the profile pattern downslope, the absolute water-table height values, and the water-table peak timings. The modelled water-table profiles show a similar pattern to those noted in the observed water-table profiles with consistent attenuation of the profile's downslope in the correct order, which was typical across both hardware models. However, the absolute values do not fit the observed data as well, with water-table peaks differing from the observed, where some over-predict water-table rise (e.g., wells50-125 in scenario 2 of the fen model – Figure 4.7) and some under-predict water-table rise (e.g., wells0-75 in scenario 2 of the bog model – Figure 4.5). The differences here are perhaps a result of the draining of the initial condition prior to each run, resulting in different model starting conditions in the wells than in the observed data. Furthermore, the negligible water-table rise in the most downslope well (well150 - particularly in scenarios 1, 3 and 4, for both sites), is likely the result of the water table being in the high *K* layers (around the NS) and so water quickly runs off to the boundary, meaning any water-table rise is small. The lag between the observed and modelled outputs noted above is also noted here and is particularly clear at

the downslope end. Despite the discrepancies between the observed and modelled water tables shown here, the overall pattern is the same for both models, with scenario 2 having the slowest responses to the input, followed by scenarios 1, 3 and 4. Therefore, the models are capable of replicating the observed water tables and follow the same pattern, but further work is required to improve replication of the starting condition and account for the lag.

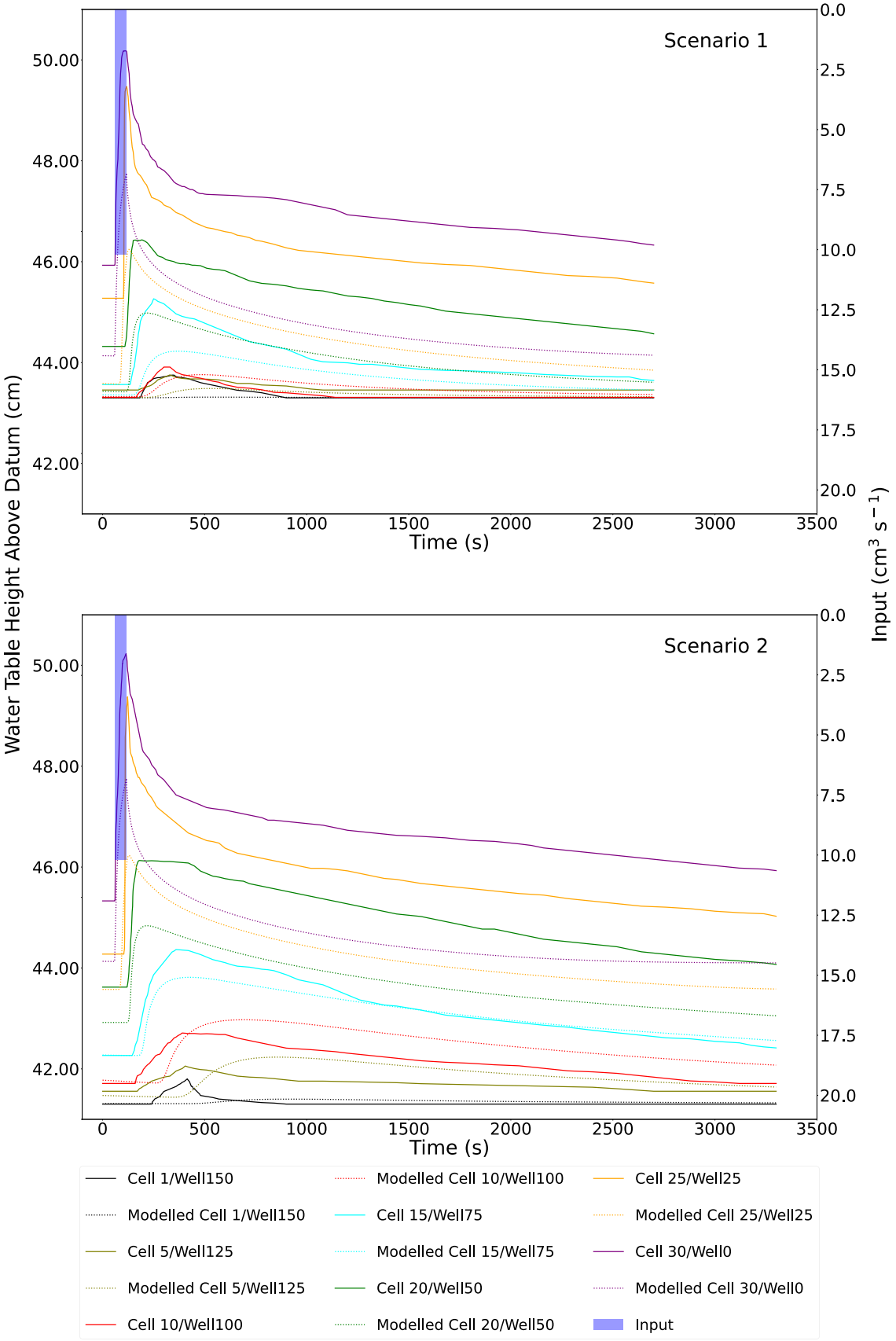

Figure 4.5. Observed and modelled water-table profiles for the bog model (median hydrograph simulations) for scenarios 1 and 2. Well0 is upslope, well150 is downslope.

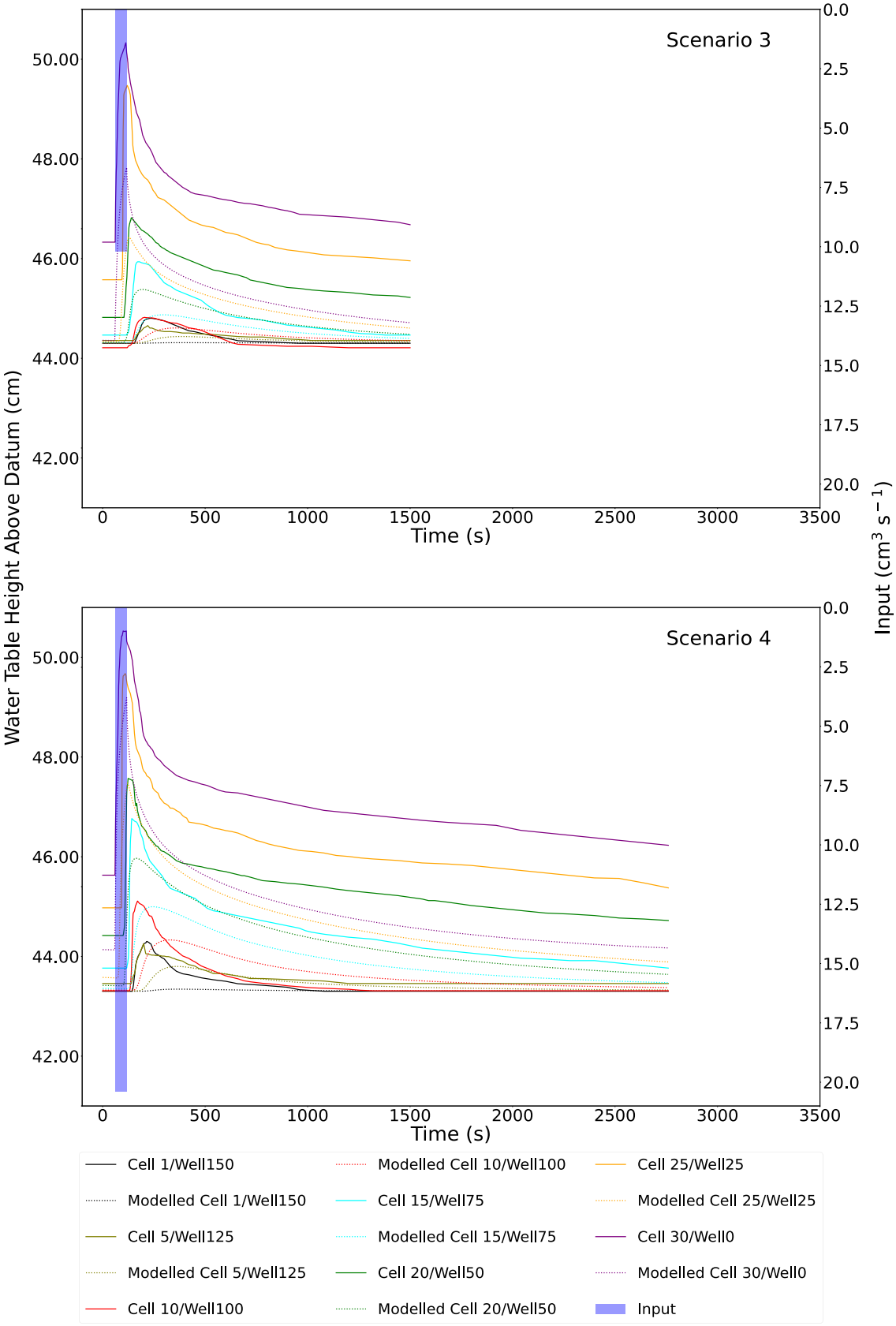

Figure 4.6. Observed and modelled water-table profiles for the bog model (median hydrograph simulations) for scenarios 3 and 4. Well0 is upslope, well150 is downslope.

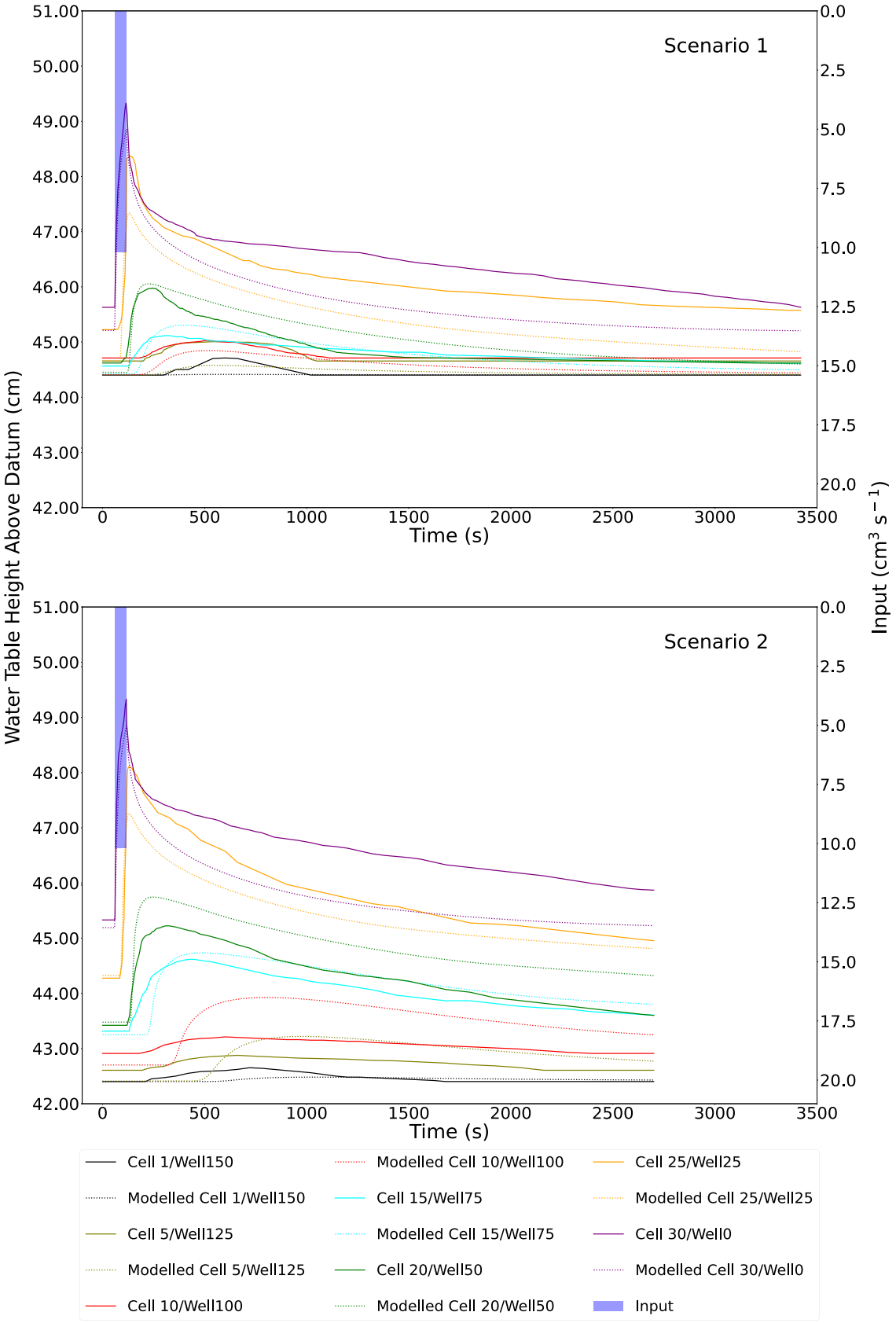

Figure 4.7. Observed and modelled water-table profiles for the fen model (median hydrograph simulations) for scenarios 1 and 2. Well0 is upslope, well150 is downslope.

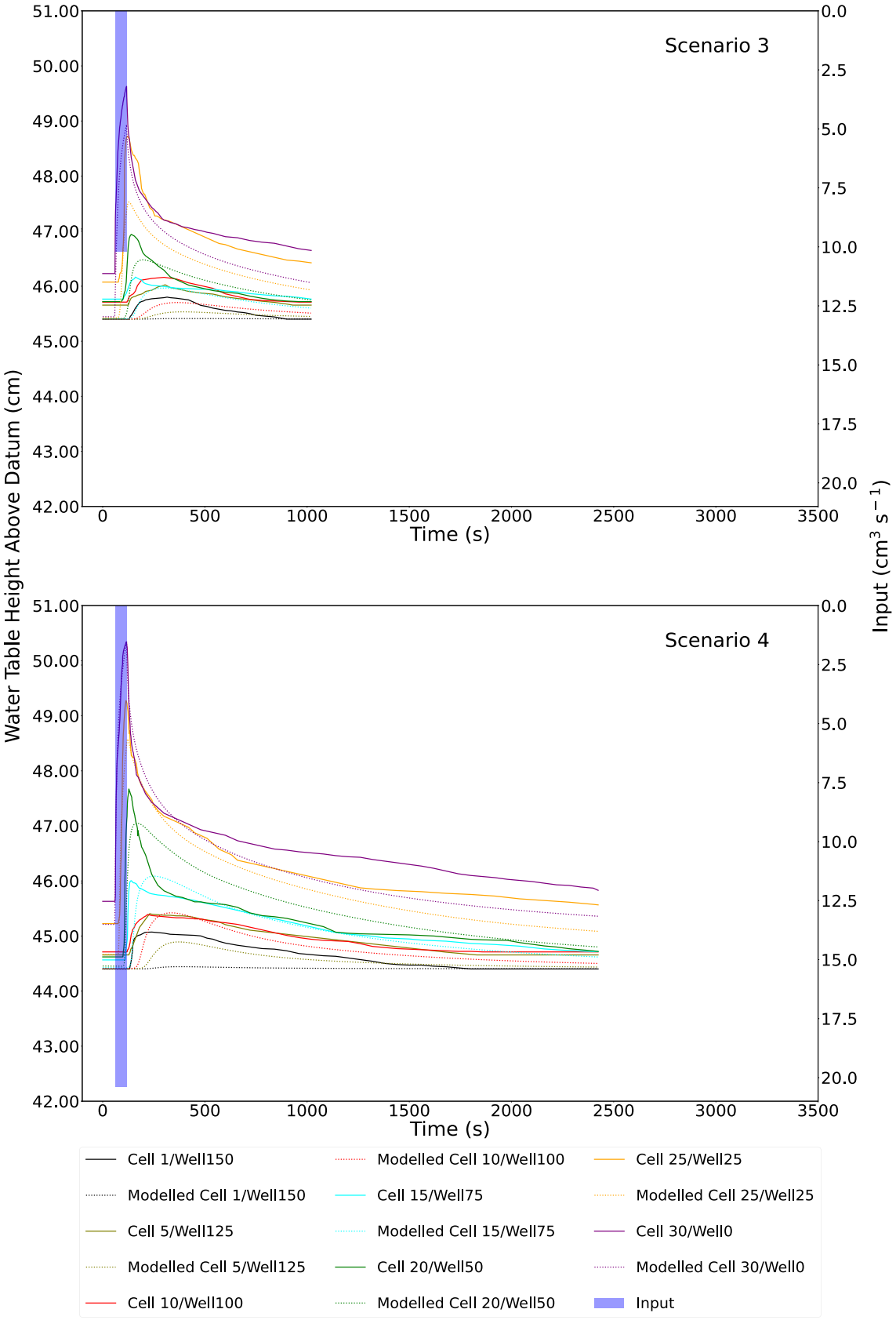

Figure 4.8. Observed and modelled water-table profiles for the fen model (median hydrograph simulations) for scenarios 3 and 4. Well0 is upslope, well150 is downslope.

4.3. Comparison of discharge between peat types

When comparing the median hydrographs, there is little difference between peat types for scenarios 1-3 in the hardware models (Figure 4.9; Table 4.1). Peak discharges between peat type are comparable for these scenarios with lag times and hydrograph shapes also being similar, bar for scenario 2 where the fen model produced a more delayed discharge peak and attenuated recessional limb. For scenario 4, the lag times are similar but the peak discharge in the bog model is nearly double that of the fen model and the hydrograph is near-symmetrical, with rapid recession. The hydrograph areas between peat types are also comparable with the largest difference being for scenario 3 (12.64%) (Table 4.2), this may be a result of different run times; however. As a whole, these data show that for both peat types, scenarios 3 and 4 produced the flashiest response to input, with steeper hydrographs and short lag times, followed by scenarios 1 and 2 where the hydrographs are much more attenuated and lag times are longer. Like the observed data, similarities can be drawn from the modelled outputs, with the modelled bog hydrographs displaying similar metrics to their fen counterparts (Table 4.1) but variable hydrograph areas (Tables 4.2).

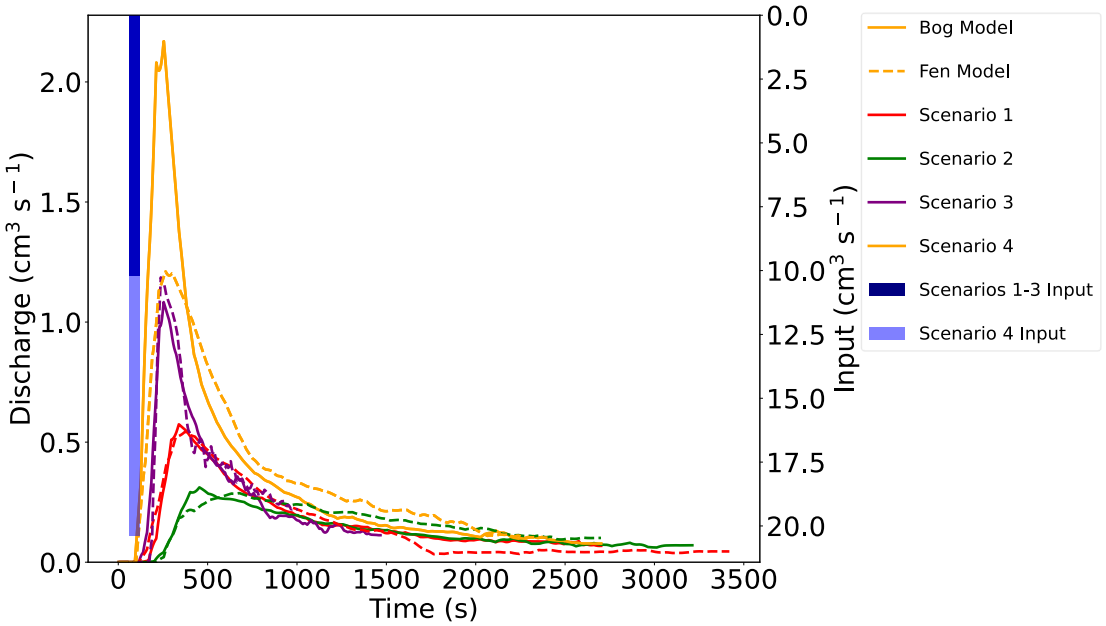

Figure 4.9. Median (peak) discharge hydrographs for each scenario and site (bog = solid line; fen = dashed line).

5. Discussion

The aim of this study was to determine if a Darcian model could be used to model a blanket peatland slope, where there is not a distinct surface but rather a thick transition zone (of tangled vegetation), using a single representation of flow instead of a coupled model. Scenarios were devised to capture flow in the transition zone. The results show that the Darcian treatment for this rapid near-surface flow does work and produces sensible results that share similarities with the observed data from the hardware models. This good fit is shown by the comparable peak discharges for the scenarios and the similar hydrograph shapes, as described in the results section. However, there is discrepancy between the modelled and observed lag times and differences between the absolute water-table height values. These are discussed below.

5.1. Rapid near-surface and transition zone flow in the hardware model

The scenarios presented in the methods and results sections clearly demonstrate the impact that flow in the near-surface and transition zone at the top of the soil column has on overall discharge and input signal transformation down a slope, with the scenarios where the water levels rose the highest creating the flashiest hydrographs. The data show that scenarios 3 and 4, where the initial condition was set to 1 cm above the NS and to the NS, but the input was double that of the other scenarios, respectively, showed the most rapid response to the input. The discharge hydrographs and water-table profiles for these scenarios responded quickly with peaky rises and falls, thus indicating toward quicker conveyance of water downslope, and corroborating the fact that runoff in the upper portion of peat results in flashy system response (Evans et al., 1999; Holden and Burt, 2003a; Holden, 2005). Scenarios 1 and 2, where the initial condition was at the NS and 2 cm below the NS respectively, produce much slower system responses to the input with more attenuated discharge hydrographs, and water-tables with

lower peaks and longer lag times, thus indicating that subsurface flow is substantially slower than that near the surface and in the transition zone. Furthermore, these data show that the starting condition, degree of saturation and input size are important with scenarios 3 and 4 showing the largest response.

The impact that depth of flow in the near-surface and transition zone has, is clear when comparing the observed discharge metrics for scenarios 1, 3 and 4 against scenario 2 (where flow was mostly subsurface). For both sites, scenario 1 produces a discharge peak that is just under double those in scenario 2, with scenario 2 having lag times that are ~1.5x longer, for the bog tank, and over twice as long for the fen tank. The difference in peak discharge and lag times grows as the depth of water increases, with the peak for scenario 3 being nearly ~3.5x larger than scenario 2 for the bog site, and over 4x larger in the fen tank. The increase in peak discharge in the fen tank between scenarios 3 and 4 is only slight compared to the bog tank, which is over double the peak for scenario 3. The bog lag times for scenarios 3 and 4 are the same and are ~76% quicker than scenario 2. Interestingly, the lag time for scenario 3 in the fen tank is shorter (~120% quicker than scenario 2) than that for scenario 4 (~108% quicker). These data largely corroborate the findings reported by Holden et al. (2008), where flow velocity increases substantially once a critical depth of vegetation submergence is reached. However, the degree of vegetation submergence was not observed in this study, so it is not known if the same process occurred here. Nevertheless, it does indicate that flows with higher water levels and greater degrees of inundation met less resistance, thus meaning flood wave conveyance, due to quasi-overland flow, is much more rapid. This rapid conveyance is supported by the water-table peak timings for each scenario, with scenarios 3 and 4 showing much faster conveyance than 1 and 2. These data further demonstrate the impact that *K* has on flow in peats, with lower *K* at depth resulting in slower flow, but also enhancing the percolation-excess and saturation-excess mechanisms that mean infiltrating water cannot percolate down and the peat fills up (Holden et

al., 2001). Furthermore, the differences in response, particularly between scenarios 2 and the others (described above) suggests that *K* substantially decreases with depth, even over the short spatial scales tested.

5.2. Effectiveness of a Darcian model

This study presents an extended Darcian model that represented the quasi-overland flow in the near-surface region using a DOLF layer; simulating flow through a highly porous mix of vegetation, similar to those in wetland environments (Kadlec, 1990; Nepf, 1999). The model proved effective at simulating flow in an environment that lacks a defined surface, shown by the good discharge fits with the observed data and the pattern of water-table profiles. By modelling the system as one entity and under one flow representation, DBH effectively simulates the saturation-excess mechanism that dominates runoff production in peat, whereby water cannot infiltrate down and the peat is filled, and so water enters the high-*K*, high-*s* near-surface and DOLF layers that simulate rapid flow in the near-surface. Moreover, the model can remain stable during the rapid flow, with the finite difference solution to the Boussinesq equation allowing the use of very small timesteps. The result is a Darcian model that can effectively simulate subsurface flow and the rapid flows that characterise peatland runoff, in an environment that lacks a defined surface.

The modelled results shown in chapter 4 demonstrate that DBH can reproduce the observed results from the hardware models and be successful at simulating near-surface flow. For example, the modelled discharge hydrographs for each scenario largely follow the same pattern as those from the hardware model, with similar overall shapes and comparable peak sizes. In particular, the model largely captures the gradients of the rising limb seen in the hardware data and whilst in most cases, the falling limb is slower than observed, the gradients are comparable. In addition, the modelled water-tables also reproduce the pattern observed in

the hardware models, but the absolute values and timings do differ. The clear discrepancy in the modelled data is the lag between hydrograph peaks and the offset of the water-table profiles. These are likely the result of the hardware model 'short-circuit', and the initial draining of the starting condition of DBH (as outlined in chapter 3). The latter results in the starting condition of DBH largely being lower than that of the hardware models, with the greatest impacts observed at the upslope end of the model and in those scenarios where the initial starting condition is high, and water is sampling the higher *K* and *s* layers. The impact of draining is less for scenario 2 where the starting levels are lower and so are sampling lower *K* and *s* layers. This is particularly clear in scenario 2 of the fen model, where the absolute values are more comparable to the observed data (with wells50, 100 and 125 overpredicting the observed data – Figure 4.7) and the initial draining of upslope wells has potentially contributed to raising the starting level in the middle section of the model (see wells0, 25 and 50 in Figure 4.7). Whilst the offset in starting condition has not had a huge impact on the fen model water-tables, the impact on the bog model is clear with the majority of wells underpredicting the absolute water-table heights for all scenarios (see Figures 4.5 and 4.6).

Despite the discrepancies in the data, the reasonable reproduction of the observed data indicate that an extended Darcian model (with a DOLF layer) is sufficient at modelling the rapid quasi-overland flow that occurs in peatlands, as a diffusive process and as one entity, meaning that explicit overland flow representations used in the past (e.g., Holden et al., 2008; Gao et al., 2015) are perhaps not required. This good reproduction of the observed data indicates that flows in the near-surface region of blanket peats are similar to those of wetland environments where flow resistance equations, such as the Manning equation, are deemed to not be appropriate due to flow being in the transition region between laminar and turbulent, which may be the case here (Kadlec, 1990). The incorporation of a DOLF layer, whilst akin to flow through vegetation on wetlands (Kadlec et al., 1981), is perhaps best applied to peatlands where

the surface is ambiguous (e.g., pristine and restored peatlands). Whereas, changes in peatland condition or land cover, for example the removal of vegetation or peat drainage (causing more concentrated flow in grips), may result in the surface being more obvious and so, these environments are possibly best modelled with more rigorous and conventional overland flow routines (Ballard et al., 2011; Gao et al., 2015; 2016).

5.3. Model lags

As noted above, there is some departure between the observed and modelled data timings. However, the lag seen in the modelled data is most likely an artefact of the hardware model, caused by the presence of discontinuous voids dispersed along the base of the peat sample resulting in preferential flow occurring between Darcian sections of peat (the 'short-circuit'), as noted in the methods section. These voids in essence shorten the tank meaning that discharge and water-table peaks are earlier than they should be. Therefore, the outputs from DBH are likely to be reasonable because of this tank short-circuiting. To show this, the bog DBH model was run again using the same setup as described in chapter 3 for scenario 1, but this time it was 20 cm shorter (shortened at the upslope end). The parameters used here were the same as those used for the results in chapter 4.

The resultant discharge hydrograph and water-tables are shown in Figures 5.1 and 5.2, respectively. Overall, these data show an improvement in the timings of the modelled peak discharge with respect to the observed discharge, supporting the suggestion made earlier. However, the predicted discharge is now greater than the observed, indicating that a new model calibration is perhaps required. Furthermore, the timings of the water-table rise in each well, bar well25 and well150 (well0 removed due to the shorter model), is also substantially improved as they are now close to matching the observed data, where before, in the results shown in chapter 4, they were displaced. On the other hand, well25 now rises slightly before its observed

counterpart, where before, the rise had a closer fit. Any rise in well150 is still negligible. Despite the improved water-table rise timings, there is still some discrepancy between the absolute values, as with the previous simulations. This discrepancy is also a likely result of initial model draining, prior to the simulations being run, creating differences in the starting water levels in the wells; however.

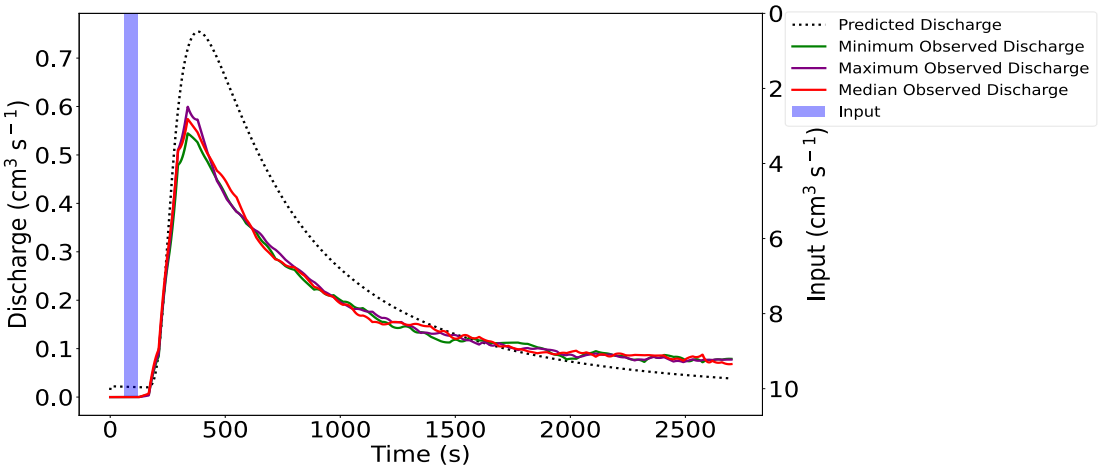

Figure 5.1. Discharge hydrograph for the shortened bog model (scenario 1).

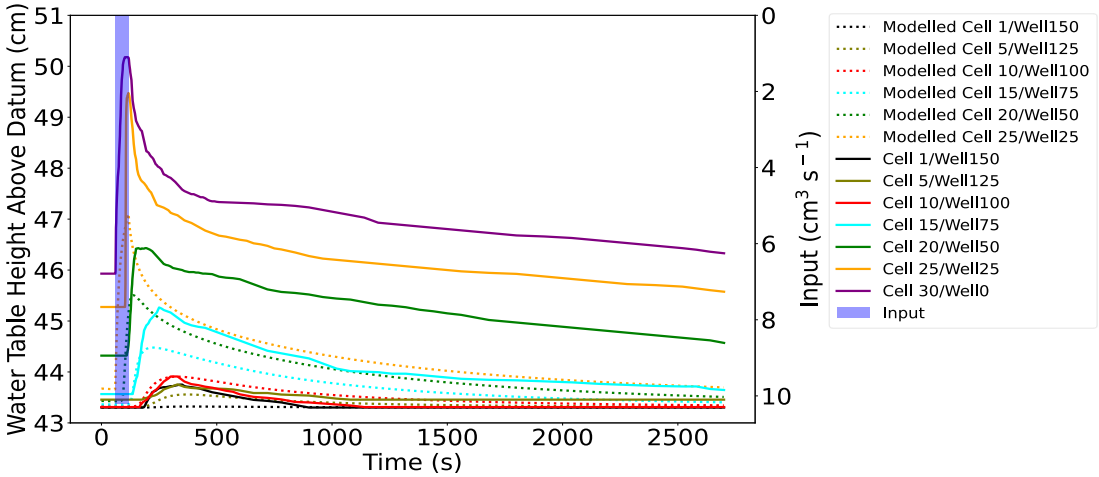

Figure 5.2. Water-table profiles for the shortened bog model (scenario 1).

5.4. Comparison of peat types

Whilst the different sites sampled from Crawshaw Moss had similar vegetation types, they varied in coverage of such vegetation. The bog site was more moss dominated (e.g., *Sphagnum* and *Polytrichum*) whilst the fen site had a greater coverage of sedges (e.g., *Eriophorum*). The properties of deep peat have clear implications for the mechanisms that lead

to the dominance of near-surface flow in peatland catchments; however, the impact that deeper peat has on stormflow itself is less relevant than the vegetation present in the near-surface region.

Holden et al. (2008) report that peatlands with predominant *Sphagnum* coverage have significantly lower overland flow velocities than those that were *Eriophorum* dominated, with those that were a mix of the two being intermediate. Despite these differences, the velocities for all treatments increased considerably with depth, once a critical depth of ~1 cm was passed (Holden et al., 2008). Moreover, on a larger scale, using the Holden et al. (2008) equation, Gao et al. (2015) found that *Sphagnum* coverage led to lower amounts of runoff compared to areas that were mostly covered by *Eriophorum*, with a similar story being found for river flow peaks (Gao et al., 2018). The likely explanation for this greater attenuation of runoff and flow by *Sphagnum* is due to its dense branching structure providing a greater roughness than other vegetation types (Holden et al., 2008). Additionally, vegetation like grasses and sedges can bend and get dragged down into the flow, reducing their effective roughness during deep flows, which may have occurred in previous studies (Freeman et al., 2000; Copeland, 2000). The bending of stems; however, was not observed during this study in both the bog and fen tanks; this is perhaps a limitation of small-scale laboratory experiments and further work is required to investigate this process. The data in chapter 4 (Figure 4.9) show that the discharge hydrographs between the samples taken for this study did not differ substantially compared to the reporting in previous studies, with similar discharge peaks and lag times demonstrated. The only exception is for scenario 4 where the peak discharge from the bog tank is substantially greater than the fen tank peak and the hydrograph is near-symmetrical with a quick falling limb. The greater discharge from the bog tank is perhaps explained by faster conveyance at various locations in the tanks, where vegetation does not protrude as high above the NS (perhaps up to +/- 1 cm difference) as that from the fen sample (where sedge stems extend above the tank). Therefore,

it is possible that more vegetation was submerged in the bog model at various points along the flume, meaning faster conveyance could occur, which may also explain the slightly shorter lag time. However, across both flumes, vegetation thickness above the NS varied (ranging between ~1-4 cm) meaning that at other locations the vegetation in the bog tank above the NS is thicker than that of the fen model, so it cannot be said with a high degree of confidence that a greater degree of submergence occurred in the bog model as a whole, thus meaning that more work on this is required. Nevertheless, the overall differences between lag times in the hydrographs and in the water-table profiles are not sizeable, indicating there was little difference in the response to an input of the peat samples used in this study. However, this study was limited by the size of the samples and that only two samples were experimented on; therefore, it is possible that if more samples of blanket peat types (with more variation) are studied, differences may be observed.

In addition, there was little difference in the parameters used between the numerical models for each site, with both models producing acceptable results. Thus, it is reasonable to suggest that the responses of both sites were fairly similar.

5.5. Further work

This study has demonstrated the effectiveness of a combined experimental and numerical modelling approach for studying peatland near-surface hydrological processes. The hardware models offer the flexibility to devise scenarios and control variables that is more difficult to achieve through an observational field approach, enabling the production of datasets to test numerical models. Through this approach, some opportunities have been identified to improve the method and for further research. These opportunities and suggestions are numbered below.

1. More samples of peat should be analysed to further improve understanding of how water flows in the peat near-surface and transition zone, with particular emphasis on looking at different types of blanket peat that have clear cut differences between them (e.g., vegetation as discussed above), whilst also investigating a greater range of flow depths in the samples.
2. Methods to mitigate the impact the voids at the base of the hardware models have should be devised to produce a more accurate representation of the system without these areas of preferential flow. These could include improving how the samples are inserted into the tank in the first place, perhaps by ensuring the base of the peat sample is flat and the sample is cut to fit the dimensions of the flume tanks more closely; and potentially drilling into the tanks where the voids are and filling these with an impermeable medium. The latter would result in an uneven tank base but may improve flow representation.
3. Video recording of the water-table wells in higher resolution would be beneficial and vastly improve the observed water-table measurements and increase confidence when making comparisons.
4. The model should be tested on degraded (and restored) blanket peatlands as these are much more common in the UK than pristine peatlands (Evans et al., 2017) and so should be targeted for further work.
5. Finally, the extended DBH model should be expanded to an entire hillslope or catchment to determine its effectiveness in modelling rapid near-surface and transition zone flow on a larger spatial scale.

5.6. Wider implications

The modelling presented in this study determines whether a Darcian diffusion-type model can be used to effectively simulate the hydrological function of the near-surface region

of a peatland hillslope. The results suggest that this modelling procedure is sufficient when simulating a system that lacks a clearly defined surface, indicating that, whilst explicit overland flow representations can simulate peatlands well, a simpler and more efficient model is perhaps more advantageous. Therefore, as noted above, DBH could be used on greater spatial scales than used in this study (e.g., landscape-scale such as a hillside or peatland catchment). The primary implication of this is that a simple single model, that uses one representation of flow, could be used to simulate peatland hydrological response to rainfall, in a manner that is less complex than a coupled model with two representations of flow, but still produces results that align with observed findings. However, empirical calibration to a peatland-fed river or stream will likely be required. If upscaling of the model is successful, it could then be used to predict the flood response of peatland catchments, which may inform flood prevention and mitigation measures.

6. Conclusion

Near-surface and surface flow mechanisms are known to be the dominant contributors to the flashy response of peatlands during storm events. So far, modelling this response has been achieved with coupled models whereby overland flow is simulated using flow resistance equations. However, whilst this is applicable to most mineral soil regions that have a distinct surface, it is perhaps not so applicable to many peatlands where the surface is ambiguous. This study suggests that the surface region of blanket peatland consists more of a transition zone that is comprised of a mix of porous undecomposed and live vegetation, similar to flow through wetlands (Kadlec et al., 1981). Using hardware models, scenarios were devised where rapid flow in this region could be simulated, and the datasets produced were used to test a numerical model. This approach was successful as it enabled flow in the near-surface to be explicitly observed in the hardware models, providing the adaptability to alter and control variables that is not likely achievable with field observation. Using these data, the numerical twins were then utilised to determine if a Darcian treatment could be used to model these flows, by comparing the two datasets.

As subsurface and acrotelm flow are modelled effectively with Darcy's law, DigiBog_Hydro was extended to include a layer which modelled quick quasi-overland flow in the near-surface and transition zone as a diffusive process. The model presented is shown to be effective at modelling rapid flows that occur in peatlands, producing discharge hydrographs that are comparable in magnitude and shape to the observed data and water-table outputs that follow the same pattern as those observed. Despite further work being required to improve the methods, and test more samples of blanket peat, these data indicate that a single representation of flow, Darcy's law, can be used for the modelling of rapid flow in the near-surface region and indicates that a simple model could be used as an alternative to coupled approaches. However,

despite the overall good replication of the observed datasets, the reason for the lag between the peak flows in the hardware and numerical models was not determined to a high degree of confidence and greater storm sizes with deeper flows and more vegetation submergence, that may be non-Darcian, were not tested. Thus, further work should involve the testing of greater ranges of flow depths and determining if the model continues to perform with deeper and higher velocity flows or if a non-Darcian representation on top of the Darcain overland flow layer is required; and to investigate if the model can be used on greater spatial scales.

7. References

Abrahams, A.D. and Parsons, A.J. 1990. Determining the mean depth of overland flow in field studies of flow hydraulics. *Water Resources Research*. **26**(3), pp.501–503.

Abrahams, A.D. and Parsons, A.J. 1991. Resistance to Overland Flow on Desert Pavement and Its Implications for Sediment Transport Modeling. *Water Resources Research*. **27**(8), pp.1827–1836.

Abrahams, A.D., Parsons, A.J. and Wainwright, J. 1994. Resistance to overland flow on semiarid grassland and shrubland hillslopes, Walnut Gulch, southern Arizona. *Journal of Hydrology*. **156**(1), pp.431–446.

Acreman, M. and Holden, J. 2013. How Wetlands Affect Floods. *Wetlands*. **33**(5), pp.773–786.

Acreman, M.C., Harding, R.J., Lloyd, C., McNamara, N.P., Mountford, J.O., Mould, D.J., Purse, B.V., Heard, M.S., Stratford, C.J. and Dury, S.J. 2011. Trade-off in ecosystem services of the Somerset Levels and Moors wetlands. *Hydrological Sciences Journal*. **56**(8), pp.1543–1565.

Ala-aho, P., Rossi, P.M., Isokangas, E. and Kløve, B. 2015. Fully integrated surface–subsurface flow modelling of groundwater–lake interaction in an esker aquifer: Model verification with stable isotopes and airborne thermal imaging. *Journal of Hydrology*. **522**, pp.391–406.

Ala-aho, P., Soulsby, C., Wang, H. and Tetzlaff, D. 2017. Integrated surface-subsurface model to investigate the role of groundwater in headwater catchment runoff generation: A minimalist approach to parameterisation. *Journal of Hydrology*. **547**, pp.664–677.

Allott, T.E.H., Auñón, J., Dunn, C., Evans, M.G., Jill, L., Paul, L., MacDonald, M., Nisbet, T., Owen, R., Pilkington, M., Proctor, S., Shuttleworth, E. and Walker, J. 2019. *Peatland Catchments and Natural Flood Management* [Online]. [Accessed 18 October 2021]. Available from: https://www.research.manchester.ac.uk/portal/.

Artz, R., Scott-Campbell, M., Chandler, D., McBride, A., Ross, K. and Weyl, R. 2019. *The State of UK Peatlands: an update* [Online]. [Accessed 2 September 2021]. Available from: https:/www.iucn-uk-peatlandprogramme.org/sites/.

Baird, A.J. 1997a. Continuity in hydrological systems. In: Wilby, R.L. ed. *Contemporary hydrology: towards holistic environmental science*. Chichester: Wiley, pp.25–58.

Baird, A.J. 1997b. Field Estimation of Macropore Functioning and Surface Hydraulic Conductivity in a Fen Peat. *Hydrological Processes*. **11**(3), pp.287–295.

Baird, A.J., Beckwith, C.W. and Heathwaite, A.L. 1997. Water movement in undamaged blanket peats. In: Tallis, J.H., Meade, R. and Hulme, P.D. (eds). *Blanket Mire Degradation: causes, consequences and challenges.* London: British Ecological Society, pp.128-139.

Baird, A.J., Eades, P.A. and Surridge, B.W.J. 2008. The hydraulic structure of a raised bog and its implications for ecohydrological modelling of bog development. *Ecohydrology*. **1**(4), pp.289–298.

Baird, A.J., Morris, P.J. and Belyea, L.R. 2012. The DigiBog peatland development model 1: rationale, conceptual model, and hydrological basis. *Ecohydrology*. **5**(3), pp.242–255.

Baird, A.J. and Waldron, S. 2003. Shallow horizontal groundwater flow in peatlands is reduced by bacteriogenic gas production. *Geophysical Research Letters*. **30**(20), article no: 2043.

Ballard, C.E., McIntyre, N., Wheater, H.S., Holden, J. and Wallage, Z.E. 2011. Hydrological modelling of drained blanket peatland. *Journal of Hydrology*. **407**(1), pp.81–93.

Barthel, R. 2014. Integration of groundwater and surface water research: an interdisciplinary problem? *Hydrol. Earth Syst. Sci.* **18**, pp.2615–2628.

Barthel, R. and Banzhaf, S. 2016. Groundwater and Surface Water Interaction at the Regional-scale-A Review with Focus on Regional Integrated Models. *Water Resources Management*. **30**, pp.1–32.

Beckwith, C.W. and Baird, A.J. 2001. Effect of biogenic gas bubbles on water flow through poorly decomposed blanket peat. *Water Resources Research*. **37**(3), pp.551–558.

Beckwith, C.W., Baird, A.J. and Heathwaite, A.L. 2003a. Anisotropy and depth-related heterogeneity of hydraulic conductivity in a bog peat. I: laboratory measurements. *Hydrological Processes*. **17**(1), pp.89–101.

Beckwith, C.W., Baird, A.J. and Heathwaite, A.L. 2003b. Anisotropy and depth-related heterogeneity of hydraulic conductivity in a bog peat. II: modelling the effects on groundwater flow. *Hydrological Processes*. **17**(1), pp.103–113.

Bennett, S.J., Ashmore, P. and Neuman, C.M. 2015. Transformative geomorphic research using laboratory experimentation. *Geomorphology*. **244**, pp.1–8.

Beven, K. 1997. TOPMODEL: A critique. *Hydrological Processes*. **11**(9), pp.1069–1085.

Beven, K. and Freer, J. 2001a. A dynamic TOPMODEL. *Hydrological Processes*. **15**(10), pp.1993–2011.

Beven, K. and Freer, J. 2001b. Equifinality, data assimilation, and uncertainty estimation in mechanistic modelling of complex environmental systems using the GLUE methodology. *Journal of Hydrology*. **249**(1), pp.11–29.

Beven, K.J. and Kirkby, M.J. 1979. A physically based, variable contributing area model of basin hydrology / Un modèle à base physique de zone d'appel variable de l'hydrologie du bassin versant. *Hydrological Sciences Bulletin*. **24**(1), pp.43–69.

Bond, S., Kirkby, M.J., Johnston, J., Crowle, A. and Holden, J. 2020. Seasonal vegetation and management influence overland flow velocity and roughness in upland grasslands. *Hydrological Processes*. **34**(18), pp.3777–3791.

Bragg, O.M. 2002. Hydrology of peat-forming wetlands in Scotland. *Science of The Total Environment*. **294**(1), pp.111–129.

Brown, L.E., Holden, J., Palmer, S.M., Johnston, K., Ramchunder, S.J. and Grayson, R. 2015. Effects of fire on the hydrology, biogeochemistry, and ecology of peatland river systems. *Freshwater Science*. **34**(4), pp.1406–1425.

Burt, T.P. 1992. The hydrology of headwater catchments. In: Calow, P. and Petts, G.E. (eds). *Rivers Handbook, 1.* Oxford: Blackwell, pp.3–28.

Burt, T.P. 1995. The role of wetlands in runoff generation from headwater catchments. In: Hughes, J. and Heathwaite, L. (eds). *Hydrology and hydrochemistry of British wetlands*. Chichester: Wiley, pp.21–38.

Charman, D.J. 1992. Blanket mire formation at the Cross Lochs, Sutherland, northern Scotland. *Boreas*. **21**(1), pp.53–72.

Charman, D.J. 1995. Patterned fen development in northern Scotland: Hypothesis testing and comparison with ombrotrophic blanket peats. *Journal of Quaternary Science*. **10**(4), pp.327–342.

Chen, L., Sela, S., Svoray, T. and Assouline, S. 2013. The role of soil-surface sealing, microtopography, and vegetation patches in rainfall-runoff processes in semiarid areas. *Water Resources Research*. **49**(9), pp.5585–5599.

Choi, J. and Harvey, J.W. 2014. Relative Significance of Microtopography and Vegetation as Controls on Surface Water Flow on a Low-Gradient Floodplain. *Wetlands*. **34**(1), pp.101–115.

Clymo, R.S. 2004. Hydraulic conductivity of peat at Ellergower Moss, Scotland. *Hydrological Processes*. **18**(2), pp.261–274.

Clymo, R.S. and Bryant, C.L. 2008. Diffusion and mass flow of dissolved carbon dioxide, methane, and dissolved organic carbon in a 7-m deep raised peat bog. *Geochimica et Cosmochimica Acta*. **72**(8), pp.2048–2066.

Copeland, R.R. 2000. *Determination of Flow Resistance Coefficients Due to Shrubs and Woody Vegetation* [Online]. Vicksburg MS: Engineer Research and Development Centre: Coastal and Hydraulics Lab. [Accessed 16 October 2021]. Available from: https://apps.dtic.mil/sti/.

Couwenberg, J., Thiele, A., Tanneberger, F., Augustin, J., Bärisch, S., Dubovik, D., Liashchynskaya, N., Michaelis, D., Minke, M., Skuratovich, A. and Joosten, H. 2011. Assessing greenhouse gas emissions from peatlands using vegetation as a proxy. *Hydrobiologia*. **674**(1), pp.67–89.

Crompton, O., Katul, G.G. and Thompson, S. 2020. Resistance Formulations in Shallow Overland Flow Along a Hillslope Covered With Patchy Vegetation. *Water Resources Research*. **56**(5), e2020WR027194.

Crompton, O., Sytsma, A. and Thompson, S. 2019. Emulation of the Saint Venant Equations Enables Rapid and Accurate Predictions of Infiltration and Overland Flow Velocity on Spatially Heterogeneous Surfaces. *Water Resources Research*. **55**(8), pp.7108–7129.

Crompton, O.V. and Thompson, S.E. 2021. Sensitivity of dryland vegetation patterns to storm characteristics. *Ecohydrology*. **14**(2), e2269.

Cunliffe, A.M., Baird, A.J. and Holden, J. 2013. Hydrological hotspots in blanket peatlands: Spatial variation in peat permeability around a natural soil pipe. *Water Resources Research*. **49**(9), pp.5342–5354.

Daniels, S.M., Agnew, C.T., Allott, T.E.H. and Evans, M.G. 2008. Water table variability and runoff generation in an eroded peatland, South Pennines, UK. *Journal of Hydrology*. **361**(1–2), pp.214–226.

Dingman, S.L. 1994. *Physical Hydrology*. New Jersey: Prentice-Hall.

Dubuc, Y., Janneteau, P., Labonté, R., Roy, C. and Brière, F. 1986. Domestic Wastewater Treatment by Peatlands in a Northern Climate: A Water Quality Study. *JAWRA Journal of the American Water Resources Association*. **22**(2), pp.297–303.

Dunkerley, D. 2001. Estimating the mean speed of laminar overland flow using dye injection-uncertainty on rough surfaces. *Earth Surface Processes and Landforms*. **26**(4), pp.363–374.

Dunkerley, D. 2018. How is overland flow produced under intermittent rain? An analysis using plot-scale rainfall simulation on dryland soils. *Journal of Hydrology*. **556**, pp.119–130.

Dunkerley, D. 2002. Volumetric displacement of flow depth by obstacles, and the determination of friction factors in shallow overland flows. *Earth Surface Processes and Landforms*. **27**(2), pp.165–175.

Dunkerley, D., Domelow, P. and Tooth, D. 2001. Frictional retardation of laminar flow by plant litter and surface stones on dryland surfaces: A laboratory study. *Water Resources Research*. **37**(5), pp.1417–1423.

Evans, C., Artz, R., Moxley, J., Taylor, E., Archer, N., Burden, A., Williamson, J., Donnelly, D., Thomson, A., Buys, G., Malcolm, H., Wilson, D. and Potts, J. 2017. *Implementation of an Emissions Inventory for UK Peatlands. Report to the Department for Business, Energy and Industrial Strategy.* Bangor: Centre for Ecology and Hydrology.

Evans, C.D., Peacock, M., Baird, A.J., Artz, R.R.E., Burden, A., Callaghan, N., Chapman, P.J., Cooper, H.M., Coyle, M., Craig, E., Cumming, A., Dixon, S., Gauci, V., Grayson, R.P., Helfter, C., Heppell, C.M., Holden, J., Jones, D.L., Kaduk, J., Levy, P., Matthews, R.A., McNamara, N.P., Misselbrook, T.H., Okley, S., Page, S.E., Rayment, M., Ridley, L.M., Stanley, K.M., Williamson, J.L., Worrall, F. and Morrison, R. 2021. Overriding water table control on managed peatland greenhouse gas emissions. *Nature*. **593**, pp.548–552.

Evans, M.G., Burt, T.P., Holden, J. and Adamson, J.K. 1999. Runoff generation and water table fluctuations in blanket peat: evidence from UK data spanning the dry summer of 1995. *Journal of Hydrology*. **221**(3–4), pp.141–160.

Evans, M.G. and Warburton, J. 2007. *Geomorphology of Upland Peat: Erosion, Form and Landscape Change*. Oxford: Blackwell Publishing.

Faybishenko, B.A. 1995. Hydraulic Behavior of Quasi-Saturated Soils in the Presence of Entrapped Air: Laboratory Experiments. *Water Resources Research*. **31**(10), pp.2421–2435.

Freeman, G.E., Rahmeyer, W.H. and Copeland, R.R. 2000. *Determination of resistance due to shrubs and woody vegetation* [Online]. Vicksburg MS: Engineer Research and Development Centre: Coastal and Hydraulics Lab. [Accessed 16 October 2021]. Available from: https://erdc-library.erdc.dren.mil/jspui/.

Frei, S. and Fleckenstein, J.H. 2014. Representing effects of micro-topography on runoff generation and sub-surface flow patterns by using superficial rill/depression storage height variations. *Environmental Modelling & Software*. **52**, pp.5–18.

Frei, S., Lischeid, G. and Fleckenstein, J.H. 2010. Effects of micro-topography on surface–subsurface exchange and runoff generation in a virtual riparian wetland — A modelling study. *Advances in Water Resources*. **33**(11), pp.1388–1401.

Frolking, S. and Roulet, N.T. 2007. Holocene radiative forcing impact of northern peatland carbon accumulation and methane emissions. *Global Change Biology*. **13**(5), pp.1079–1088.

Gao, J., Holden, J. and Kirkby, M. 2015. A distributed TOPMODEL for modelling impacts of land-cover change on river flow in upland peatland catchments. *Hydrological Processes*. **29**(13), pp.2867–2879.

Gao, J., Holden, J. and Kirkby, M. 2017. Modelling impacts of agricultural practice on flood peaks in upland catchments: An application of the distributed TOPMODEL. *Hydrological Processes*. **31**(23), pp.4206–4216.

Gao, J., Holden, J. and Kirkby, M. 2016. The impact of land-cover change on flood peaks in peatland basins. *Water Resources Research*. **52**(5), pp.3477–3492.

Gao, J., Kirkby, M. and Holden, J. 2018. The effect of interactions between rainfall patterns and land-cover change on flood peaks in upland peatlands. *Journal of Hydrology*. **567**, pp.549–559.

Garneau, M., Baird, A.J., Morris, P.J. and van Bellen, S. 2016. Testing a new version of the DigiBog model to explore the differential response of peatland microforms to shifts in surface wetness. In: *EGU General Assembly Conference Abstracts* [Online]. [Accessed 17 August 2021]. Available from: https://ui.adsabs.harvard.edu/abs/.

Gorham, E. 1991. Northern Peatlands: Role in the Carbon Cycle and Probable Responses to Climatic Warming. *Ecological Applications*. **1**(2), pp.182–195.

Grayson, R., Holden, J. and Rose, R. 2010. Long-term change in storm hydrographs in response to peatland vegetation change. *Journal of Hydrology*. **389**(3), pp.336–343.

Harbaugh, A.W. and McDonald, M.G. 1996. *User's documentation for MODFLOW-96, an update to the U.S. Geological Survey modular finite-difference ground-water flow model* [Online]. Virginia: U.S. Geological Survey. [Accessed 10 February 2021]. Available from: https://pubs.er.usgs.gov/publication/ofr96485.

Holden, J. and Burt, T.P. 2002a. Piping and pipeflow in a deep peat catchment. *Catena*. **48**(3), pp.163–199.

Holden, J. 2017. *An introduction to physical geography and the environment.* 4th ed. Harlow: Pearson.

Holden, J. 2006. Chapter 14 Peatland hydrology. *Developments in Earth Surface Processes*. **9**, pp.319–346.

Holden, J. 2009. Flow through macropores of different size classes in blanket peat. *Journal of Hydrology*. **364**(3–4), pp.342–348.

Holden, J. 2005. Peatland hydrology and carbon release: why small-scale process matters. *Philosophical Transactions of the Royal Society A: Mathematical, Physical and Engineering Sciences*. **363**(1837), pp.2891–2913.

Holden, J. and Burt, T.P. 2003b. Hydraulic conductivity in upland blanket peat: measurement and variability. *Hydrological Processes*. **17**(6), pp.1227–1237.

Holden, J. and Burt, T.P. 2003c. Hydrological studies on blanket peat: the significance of the acrotelm-catotelm model. *Journal of Ecology*. **91**(1), pp.86–102.

Holden, J. and Burt, T.P. 2002b. Infiltration, runoff and sediment production in blanket peat catchments: implications of field rainfall simulation experiments. *Hydrological Processes*. **16**(13), pp.2537–2557.

Holden, J. and Burt, T.P. 2003a. Runoff production in blanket peat covered catchments. *Water Resources Research*. **39**(7), article no: 1191.

Holden, J., Burt, T.P. and Cox, N.J. 2001. Macroporosity and infiltration in blanket peat: the implications of tension disc infiltrometer measurements. *Hydrological Processes*. **15**(2), pp.289–303.

Holden, J., Kirkby, M.J., Lane, S.N., Milledge, D.G., Brookes, C.J., Holden, V. and McDonald, A.T. 2008. Overland flow velocity and roughness properties in peatlands. *Water Resources Research*. **44**(6), article no: W06415.

Horton, R.E. 1945. Erosional development of streams and their drainage basins; hydrophysical approach to quantitative morphology. *GSA Bulletin*. **56**(3), pp.275–370.

Horton, R.E. 1933. The role of infiltration in the hydrologic cycle. *Transactions-American Geophysical Union*. **14**(1), pp.446–460.

Hubbert, M.K. 1957. Darcy's Law and the field equations of the flow of underground fluids. *Hydrological Sciences Journal*. **2**(1), pp.23–59.

Ingram, H.A.P. 1978. Soil layers in mires: function and terminology. *Journal of Soil Science*. **29**(2), pp.224–227.

Kadlec, R.H. 1990. Overland Flow in Wetlands: Vegetation Resistance. *Journal of Hydraulic Engineering*. **116**(5), pp.691–706.

Kadlec, R.H., Hammer, D.E., Nam, I.-S. and Wilkes, J.O. 1981. The Hydrology of Overland Flow in Wetlands. *Chemical Engineering Communications*. **9**(1–6), pp.331–344.

Kleinhans, M.G., Bierkens, M.F.P. and van der Perk, M. 2010. HESS Opinions On the use of laboratory experimentation: 'Hydrologists, bring out shovels and garden hoses and hit the dirt'. *Hydrology and Earth System Sciences*. **14**(2), pp.369–382.

Lai, S.Y.J., Gerber, T.P. and Amblas, D. 2016. An experimental approach to submarine canyon evolution. *Geophysical Research Letters*. **43**(6), pp.2741–2747.

Lane, S.N. and Milledge, D.G. 2013. Impacts of upland open drains upon runoff generation: a numerical assessment of catchment-scale impacts. *Hydrological Processes*. **27**(12), pp.1701–1726.

Lapen, D.R., Price, J.S. and Gilbert, R. 2005. Modelling two-dimensional steady-state groundwater flow and flow sensitivity to boundary conditions in blanket peat complexes. *Hydrological Processes*. **19**(2), pp.371–386.

Leifeld, J., Wüst-Galley, C. and Page, S. 2019. Intact and managed peatland soils as a source and sink of GHGs from 1850 to 2100. *Nature Climate Change*. **9**(12), pp.945–947.

Leonard, L.A. and Luther, M.E. 1995. Flow hydrodynamics in tidal marsh canopies. *Limnology and Oceanography*. **40**(8), pp.1474–1484.

Lewis, C., Albertson, J., Xu, X. and Kiely, G. 2012. Spatial variability of hydraulic conductivity and bulk density along a blanket peatland hillslope. *Hydrological Processes*. **26**(10), pp.1527–1537.

Lewis, C., Albertson, J., Zi, T., Xu, X. and Kiely, G. 2013. How does afforestation affect the hydrology of a blanket peatland? A modelling study. *Hydrological Processes*. **27**(25), pp.3577–3588.

Marinas, M. 2009. *The effects of disconnected entrapped air on hydraulic conductivity in the presence of water table fluctuations.*[Online] Master of Science, Hamilton: McMaster University. Available from: https://macsphere.mcmaster.ca/handle/11375/9054.

McWhorter, D.B. and Sunada, D.K. 1977. *Ground-water Hydrology and Hydraulics*. Highlands Ranch, CO: Water Resources Publication.

Metcalfe, P., Beven, K. and Freer, J. 2015. Dynamic TOPMODEL: A new implementation in R and its sensitivity to time and space steps. *Environmental Modelling & Software*. **72**, pp.155–172.

Morris, P.J., Baird, A.J. and Belyea, L.R. 2012. The DigiBog peatland development model 2: ecohydrological simulations in 2D. *Ecohydrology*. **5**(3), pp.256–268.

Morris, P.J., Baird, A.J., Young, D.M. and Swindles, G.T. 2015. Untangling climate signals from autogenic changes in long-term peatland development. *Geophysical Research Letters*. **42**(24), 10,788-10,797.

Morris, P.J., Waddington, J.M., Benscoter, B.W. and Turetsky, M.R. 2011. Conceptual frameworks in peatland ecohydrology: looking beyond the two-layered (acrotelm-catotelm) model. *Ecohydrology*. **4**(1), pp.1–11.

Mueller, E.N., Wainwright, J. and Parsons, A.J. 2007. Impact of connectivity on the modeling of overland flow within semiarid shrubland environments. *Water Resources Research*. **43**(9), article no: W09412.

Natural England, 2010. *England's peatlands: carbon storage and greenhouse gases - NE257* [Online]. [Accessed 20 November 2020]. Available from: http://publications.naturalengland.org.uk/publication/30021.

Nepf, H., Ghisalberti, M., White, B. and Murphy, E. 2007. Retention time and dispersion associated with submerged aquatic canopies. *Water Resources Research*. **43**(4), article no: W04422.

Nepf, H.M. 1999. Drag, turbulence, and diffusion in flow through emergent vegetation. *Water Resources Research*. **35**(2), pp.479–489.

Ogawa, H. and Male, J.W. 1986. Simulating the Flood Mitigation Role of Wetlands. *Journal of Water Resources Planning and Management*. **112**(1), pp.114–128.

Page, S.E. and Baird, A.J. 2016. Peatlands and Global Change: Response and Resilience. *Annual Review of Environment and Resources*. **41**(1), pp.35–57.

Parry, L.E., Chapman, P.J., Palmer, S.M., Wallage, Z.E., Wynne, H. and Holden, J. 2015. The influence of slope and peatland vegetation type on riverine dissolved organic carbon and water colour at different scales. *Science of The Total Environment*. **527–528**, pp.530–539.

Parry, L.E., Charman, D.J. and Noades, J.P.W. 2012. A method for modelling peat depth in blanket peatlands. *Soil Use and Management*. **28**(4), pp.614–624.

Parsons, A.J., Wainwright, J., Abrahams, A.D. and Simanton, J.R. 1997. Distributed dynamic modelling of interrill overland flow. *Hydrological Processes*. **11**(14), pp.1833–1859.

Pechlivanidis, I., Jackson, B., McIntyre, N. and Wheater, H. 2011. Catchment scale hydrological modelling: a review of model types, calibration approaches and uncertainty analysis methods in the context of recent developments in technology and applications. *Global NEST*. **13**(3), pp.193–214.

Price, J.S. 1992. Blanket bog in Newfoundland. Part 2. Hydrological processes. *Journal of Hydrology*. **135**(1), pp.103–119.

Reeve, A.S., Siegel, D.I. and Glaser, P.H. 2000. Simulating vertical flow in large peatlands. *Journal of Hydrology*. **227**(1), pp.207–217.

Rosenberry, D.O., Glaser, P.H. and Siegel, D.I. 2006. The hydrology of northern peatlands as affected by biogenic gas: current developments and research needs. *Hydrological Processes*. **20**(17), pp.3601–3610.

Rydin, H. and Jeglum, J.K. 2006. *The Biology of Peatlands*. Oxford: Oxford University Press.

Scoging, H. 1992. Modelling overland-flow hydrology for dynamic hydraulics. In: Parsons, A.J. and Abrahams, A.D. (eds). *Overland flow: hydraulics and erosion mechanics*. London: UCL Press, pp.81–96.

Scoging, H., Parsons, A.J. and Abrahams, A.D. 1992. Application of a dynamic overland-flow hydraulic model to a semi-arid hillslope, Walnut Gulch, Arizona. In: Parsons, A.J. and Abrahams, A.D. (eds). *Overland flow: hydraulics and erosion dynamics*. London: UCL Press, pp.96–137.

Seeger, M., Quinton, J. and Kuhn, N.J. 2012. Experiments in Earth surface process research. *Catena*. **91**, pp.1–3.

Skaggs, R.W., Fausey, N. and Nolte, B. 1981. Water Management Model Evaluation for North Central Ohio. *Transactions of the ASAE*. **24**(4), pp.0922–0928.

Smart, R.P., Holden, J., Dinsmore, K.J., Baird, A.J., Billett, M.F., Chapman, P.J. and Grayson, R. 2012. The dynamics of natural pipe hydrological behaviour in blanket peat. *Hydrological Processes*. **27**(11), pp.1523–1534.

Smith, M.W., Cox, N.J. and Bracken, L.J. 2007. Applying flow resistance equations to overland flows. *Progress in Physical Geography: Earth and Environment*. **31**(4), pp.363–387.

Thompson, S., Katul, G., Konings, A. and Ridolfi, L. 2011. Unsteady overland flow on flat surfaces induced by spatial permeability contrasts. *Advances in Water Resources*. **34**(8), pp.1049–1058.

Tiemeyer, B., Albiac Borraz, E., Augustin, J., Bechtold, M., Beetz, S., Beyer, C., Drösler, M., Ebli, M., Eickenscheidt, T., Fiedler, S., Förster, C., Freibauer, A., Giebels, M., Glatzel, S., Heinichen, J., Hoffmann, M., Höper, H., Jurasinski, G., Leiber-Sauheitl, K., Peichl-Brak, M., Roßkopf, N., Sommer, M. and Zeitz, J. 2016. High emissions of greenhouse gases from grasslands on peat and other organic soils. *Global Change Biology*. **22**(12), pp.4134–4149.

Turetsky, M.R., Kotowska, A., Bubier, J., Dise, N.B., Crill, P., Hornibrook, E.R.C., Minkkinen, K., Moore, T.R., Myers-Smith, I.H., Nykänen, H., Olefeldt, D., Rinne, J., Saarnio, S., Shurpali, N., Tuittila, E.-S., Waddington, J.M., White, J.R., Wickland, K.P. and Wilmking, M. 2014. A synthesis of methane emissions from 71 northern, temperate, and subtropical wetlands. *Global Change Biology*. **20**(7), pp.2183–2197.

Turunen, J., Tolonen, K. and Reinikainen, A. 2001. Estimating carbon accumulation rates of undrained mires in Finland—Application to boreal and subarctic regions. *The Holocene*. **12**(1), pp.69–80.

UKCEH n.d. *Peatlands factsheet* [Online]. UK Centre for Ecology and Hydrology. [Accessed 23 November 2020]. Available from: https://www.ceh.ac.uk/factsheets.

University of Leeds Peat Club, Bacon, K.L., Baird, A.J., Blundell, A., Bourgault, M.-A., Chapman, P.J., Dargie, G., Dooling, G.P., Gee, C., Holden, J., Kelly, T.J., McKendrick-Smith, K.A., Morris, P.J., Noble, A., Palmer, S.M., Quillet, A., Swindles, G.T., Watson, E.J. and Young, D.M. 2017. Questioning ten common assumptions about peatlands. *Mires and Peat*. **19**, pp.1–23.

Winter, T.C., Harvey, J.W., Franke, O.L. and Alley, W.M. 1998. *Ground Water and Surface Water: A Single Resource (U.S. Geological Survey Circular 1139)* [Online]. Denver: U.S. Geological Survey. [Accessed 15 July 2021]. Available from: https://pubs.er.usgs.gov/publication/cir1139.

Wolstenholme, J.M., Smith, M.W., Baird, A.J. and Sim, T.G. 2020. A new approach for measuring surface hydrological connectivity. *Hydrological Processes*. **34**(3), pp.538–552.

Worrall, F., Evans, M.G., Bonn, A., Reed, M.S., Chapman, D. and Holden, J. 2009. Can carbon offsetting pay for upland ecological restoration? *Science of The Total Environment*. **408**(1), pp.26–36.

Xu, J., Morris, P.J., Liu, J. and Holden, J. 2018. PEATMAP: Refining estimates of global peatland distribution based on a meta-analysis. *Catena.* **160**, pp.134-140.

Young, D.M., Ramirez, J., Gill, P.J., Baird, A.J., Morris, P.J., Davies, A.L., Tipping, R. and Peleg, N. 2020. Totally topography? Assessing the resilience of blanket peatlands to climate change using Winter's concept of the 'hydrologic landscape' and the DigiBog model. In: *AGU Fall Meeting Abstracts* [Online]. AGU. [Accessed 17 August 2021]. Available from: https://agu.confex.com/agu/.

Yu, Z., Loisel, J., Brosseau, D.P., Beilman, D.W. and Hunt, S.J. 2010. Global peatland dynamics since the Last Glacial Maximum. *Geophysical Research Letters*. **37**(13), article no: L13402.